

Distributed energy management of electric vehicle charging stations based on hierarchical pricing mechanism and aggregate feasible regions

Weiqi Meng^a, Dongran Song^{a,*}, Liansheng Huang^{b,c}, Xiaojiao Chen^b, Jian Yang^a, Mi Dong^a, M. Talaat^d, M.H. Elkholy^{d,e}

^a School of Automation, Central South University, Changsha, China

^b Institute of Plasma Physics, Chinese Academy of Sciences, Hefei, China

^c University of Science and Technology of China, Hefei, China

^d Electrical Power and Machines Department, Faculty of Engineering, Zagazig University, P.O.44519, Zagazig, Egypt

^e Department of Electrical and Electronics Engineering, University of the Ryukyus, Okinawa, 903-0213, Japan

ARTICLE INFO

Handling Editor: Neven Duic

Keywords:

Electric vehicle charging station
Hierarchical pricing mechanism
Aggregate feasible region
Distributed energy management
Distribution network

ABSTRACT

With the rapid development of electric vehicle charging stations, effective management of them has become challenging due to the high uncertainty of electric vehicles, the pricing mechanisms of charging stations, and their coupling with distribution networks. To address these challenges, this paper proposes a two-stage framework for energy management at charging stations. In the first stage, a resource allocation model considering the profits of distribution systems, charging stations, and electric vehicle users is established based on the aggregate feasible power regions of charging stations. The aggregate feasible region is obtained based on the combination of Minkowski summation and the data-driven method, which can preserve the privacy of electric vehicle data and reduce the computational burden. In the second stage, a novel hierarchical pricing mechanism is developed, which encompasses both the clearing price between charging stations and distribution networks and the retail electricity price between charging stations and electric vehicle users. Notably, charging stations participate in the power clearing of distributed networks based on the aggregate feasible power region, while a two-stage robust pricing strategy is established between electric vehicle users and charging stations. The model is finally optimized through a distributed coordination mechanism with a clear physical interpretation. The simulation results show that the proposed aggregation method enables charging stations to achieve a total economic profit at least 1.76 % higher than three competitive methods. The hierarchical pricing mechanism allows charging stations to achieve total economic profits 18.60 % and 2.94 % higher than those in the centralized dispatch and price-taker modes, respectively, while simultaneously reducing operating costs for the distributed network by 25.96 % and 27.99 %.

1. Introduction

In recent years, the growing emphasis on sustainable energy usage and reducing greenhouse gas emissions has triggered an increased prevalence of electric vehicles (EVs) [1]. The rising adoption of EVs contributes to the surging need for charging stations to support them [2]. As a natural aggregator of EVs [3], the operation of charging stations enables EVs to participate in the management of the power system through equipped energy storage devices and renewable generation [4]. However, an uncoordinated EV charging schedule would further strain the power grid [5]. Haphazard charging of EVs can result in peak load

problems that compromise the overall reliability of the distribution network [6]. The authors of [2] have demonstrated that the uncoordinated charging of EVs can have a counterproductive effect on reducing carbon emissions. Therefore, a reasonable and orderly energy management plan for charging and discharging needs to be developed by charging station operators (CSOs) [7], which can enable EV users to become excellent prosumers [8].

In optimizing the energy management of CSOs, treating EVs as conventional plug-and-charge loads would waste their potential storage capacity [9]. To meet both the economic and technical requirements of CSOs, peer-to-peer (P2P) energy trading has emerged as a promising technology, allowing participants to exchange energy with each other

* Corresponding author.

E-mail address: songdongran@csu.edu.cn (D. Song).

Nomenclature	
<i>Abbreviations</i>	
EVs	Electric vehicles
DSO	Distribution system operator
CSOs	Charging station operators
PV	Photovoltaic generation
V2G	Vehicle to grid
P2P	Peer-to-peer
ADMM	Alternating direction method of multipliers
MIP	Mixed integer program
DLMP	Distributed locational marginal prices
LSOCR-OPF	Linearized second-order cone relaxation dynamic optimal power flow
TSO	Transmission system operator
BESS	Battery energy storage system
SOC	State of charge
CC&G	Column-and-constraint generation
TOU	Time of use
<i>Variables</i>	
f_{DSO}	Objective function of DSO
f_{TSO}	Cost of interacting with utility
f_{CSO_i}	Objective function of CSO_i
f_{EV_s}	Expected value of EV users' profits
f_{loss}	Loss objective function
$f_{EV_s}^{cost}$	Charging and discharging cost of EVs participating in demand response
$f_{EV_s}^{utility}$	Utility function for EVs
$E\{\cdot\}$	Mathematical expectation
λ	Price to turn the power loss into a monetary term
r_{jk}	Resistance of branch jk
\tilde{I}_{jk}	Current flowing through branch jk at time t
Ω	Number of distribution network branches
Δt	Time interval
$p_0^b(t), p_0^s(t)$	Energy bought/sold by bus 0 at time t
$\gamma_{TSO}^b, \gamma_{TSO}^s$	Utility electricity buy and sale prices
T	Total number of time intervals
N_{CSO}	Number of charging station
$f_{CSO_i}^{Day-ahead}$	Day-ahead power plan cost of CSO_i
$f_{CSO_i}^{Real-time}$	Real-time power plan cost of CSO_i
M	Number of historical data
ϵ, ρ	Accuracy tolerance, penalty parameter
θ	Tolerance value
$P_{i,t}^{ch}, P_{i,t}^{dis}$	Charging and discharging plan of CSO_i with DSO at time t
$P_{i,t}^{ch,max}, P_{i,t}^{dis,max}$	Maximum power plan of CSO_i with DSO at time t
$S_{i,t}$	Energy level of CSO_i at time t
$S_{i,t}^{max}, S_{i,t}^{min}$	Boundary of the energy level of CSO_i at time t
$\Delta S_{i,t}$	Energy change of CSO_i caused by the connection/disconnection of EVs at time t
$\eta_{ch}^{EV}, \eta_{dis}^{EV}$	Charging and discharging efficiencies of EVs
η^{ref}	Discharge replenishment coefficient, determined by the discharge loss
T_n^{ar}	Arrival time of EV_n at the charging station
T_n^{de}	Departure time of EV_n
$s_{n,ar}, s_{n,de}$	Initial and expected battery levels of EV_n upon arrival and departure
s_n^{max}, s_n^{min}	Upper and lower bounds of the battery level of EV_n
$P_{n,max}, P_{n,max}^{dis}$	Maximum charging and discharging power limits of EV_n
$\Pi_{CSO_i}^{Da}$	Day-ahead aggregate feasible region of CSO_i
$\Pi_{CSO_i}^{Re}$	Real-time aggregate feasible region of CSO_i
$a_{n,t}^{EV}$	Unit utility of EV_n at time t
$\mu_{p,i,t}^{Da}, \mu_{p,i,t}^{Re}$	Day-ahead and real-time clearing price of CSO_i at time t
$P_{b,i,t}^{Da}$	Day-ahead purchased electricity of CSO_i from the DSO at time t
$P_{s,i,t}^{Re}, P_{b,i,t}^{Re}$	Purchasing and selling electricity for CSO_i from/to the DSO in real time at time t
π_t	Retail electricity price at time t
$P_{ch,i,t}^{BESS}, P_{dis,i,t}^{BESS}$	Power schedule of the BEES for CSO_i at time t
$P_{wind,i,t}$	Power generation of wind for CSO_i at time t
$P_{pv,i,t}$	Power generation of PV for CSO_i at time t
$P_{ch,n,t}^{EV}, P_{dis,n,t}^{EV}$	Charge and discharge plan of EV_n at time t
$s_{n,t}^{EV}$	Amount of electricity consumed by EV_n at time t
σ_0	Empirical distribution of uncertain variables
σ	A vector representing σ_0
N^{EV}	Average number of EVs served by CSOs in one day
\mathcal{N}^{EV}	Collection of EVs
\mathcal{R}	The variable space of σ
N_{type}	Number of EVs in each EV set
$P_{i,t}^{ch}, P_{i,t}^{dis}$	Maximum power plan of CSO_i with DSO at time t
$P_{jk,t}^{Da}, P_{jk,t}^{Re}$	Day-ahead and real-time active power flow of the DSO in branch jk at time t
a_t^{Da}, a_t^{Re}	Sensitivity coefficient of the day-ahead and real-time electricity price at time t
$\beta_t^{Da}, \beta_t^{Re}$	Day-ahead and real-time base price at time t
ω	Confidence level
$P_{g,i,t}^k, P_{jk,t}^{k+1}$	Total transactional electricity between CSO_i and the DSO at time t
$f_{g,i}$	Revenue generated from electricity transactions with CSO_i for the DSO
$P_{jk,t}, Q_{jk,t}$	Active and reactive power flow in branch jk at time t
$\tilde{U}_{j,t}$	Voltage of node j at time t

for higher profits [10]. Non-cooperative leader-follower game based P2P schemes are adopted for facility sharing [11] and sharing among multiple PV prosumers [12]. The authors of [13] propose an energy sharing mechanism based on a generalized Nash equilibrium for prosumers represented by CSOs. Meanwhile, a novel agent-based evolutionary game model is designed in Ref. [14] to describe the relationship between CSOs and EV users. However, these non-cooperative game-based approaches may lead to suboptimal social welfare due to conflicts of interest between consumers and system operators [15]. Therefore, some scholars have proposed cooperative operating schemes [16], such as the prosumer Stackelberg model based on the cooperative mode in Ref. [17]. However, centralized schemes require the collection of private

data from charging stations for centralized scheduling [18]. In contrast, distributed optimization schemes have more advantages in terms of promotion [19] and privacy [20]. As another form of P2P energy trading [21], distributed optimization schemes have been widely applied in the field of energy system optimization [22]. The authors of [23] provide a detailed summary of the application of the alternating direction method of multipliers (ADMM) distributed algorithm in the smart grid [24]. While distributed optimization-based approaches can achieve social optimality, it is unclear why participants should follow the decision rules derived from the Lagrange function. There is still a lack of clear physical mechanism explanation for the distributed collaborative optimization of EV charging stations.

It is noteworthy that the above-mentioned studies mainly focus on optimizing the energy trading of CSOs without considering the impact of the power boundaries of the large-scale EVs and the coupling of the distribution networks on the optimization model [25]. This overlooks the aggregate feasible region of EV power as flexible loads [9] and the effect of distribution network node location on the electricity prices of CSOs [26]. However, independently modeling large-scale EVs introduces a substantial number of variables, which may lead to the energy management model not being solved in time or even being infeasible [22]. Hence, power aggregators (such as CSOs) are needed to represent and integrate EVs into grid dispatch [27]. Therefore, a rational assessment of the aggregate feasible region of EV power within the coverage area of CSOs reflects the impact of EVs on energy management [28]. At this point, the aggregate feasible region of EV power is to perform EV cluster equivalence by superimposing decision boundaries [29]. As for the research on aggregate feasible regions, it can be divided into two types based on the modeling principle: model-based [30] and data-driven [31]. The authors of [30] use precise and approximate models to characterize the power flexibility range of distributed energy. In Ref. [32], data mining and statistical methods are used to predict the charging and discharging power curves of EVs. Although the above work has achieved ideal results, the aggregate feasible power region of EV charging stations covering large-scale EVs needs to be independently studied due to the requirements for privacy and the complex characteristics of EV users. For the collaborative modeling of the distribution network, charging stations [33], and EV users [34], the authors of [26] establish a distributed coordination mechanism with a clear physical interpretation for the energy management of CSOs in the distribution network. The authors of [35] propose a novel comprehensive planning framework for the optimal configuration of renewable energy, energy storage units, and charging stations in the distribution network. Currently, there is no research on distributed energy system management modeling that simultaneously considers the aggregate feasible region of EV power within the coverage of CSOs, the demand response of EV users and EV charging stations that are restricted by the distribution network and equipped with renewable generation and energy storage [36].

Another important issue related to CSOs modeling is their economic strategy [37]. A well-developed economic strategy can be beneficial for EV users, CSOs, and the distribution system operator (DSO) [38]. The economic strategy of charging stations is reflected in the electricity price payment mechanism, which can be divided into two types: price-driven mode and event-driven mode [39]. In the price-driven mode, electricity purchasers, who act as price-takers, adjust their electricity consumption plans based on time-of-use (TOU) electricity prices [40]. For instance, a dynamic pricing strategy based on the demand response of EV users has been proposed in Ref. [41]. On the other hand, the event-driven mode primarily employs technical indicators as control signals for electricity consumption planning. For example, the authors of [42] propose a decentralized congestion management framework for CSOs targeting DSO congestion issues. However, TOU electricity pricing may not guarantee the stability of the electricity market and power system [43]. The event-driven mode requires high prediction accuracy [44]. One potential solution is to design a hierarchical pricing mechanism that ensures fair transactions among the DSO, CSOs, and EV users while avoiding grid congestion and the scarcity of EV charging resources. In this regard, the authors of [45] introduce a cost-sharing payment mechanism to incentivize EV aggregators to participate in the power market through cooperation. The pricing mechanism presented in Ref. [46] prioritizes the interests of power companies, which restricts EV users' demand response. The authors of [47] consider the interests of multiple parties, including the DSO and CSOs, but their pricing scheme is not applicable to the power market clearing mechanism, and it fails to explain the impact of electricity consumption planning on the pricing mechanism. Therefore, there is an urgent need for research on a hierarchical pricing mechanism that simultaneously embodies the economic

and technical benefits of the DSO, CSOs, and EV users, while aligning with the principles of market clearing transactions [48].

Given that no previous research has considered all the above concerns in one work before, comprehensive research on the noted issues is necessary for the optimal energy management of CSOs. In this paper, a two-stage framework for energy management of EV charging stations based on the hierarchical payment mechanism and aggregate feasible power regions of CSOs is proposed. In the first stage, integrated modeling of the DSO, CSOs, and EVs is conducted based on the aggregate feasible power regions of CSOs. In the second stage, an economic strategy that embodies the hierarchical pricing mechanism is established. A distributed energy management scheme is designed within the integrated model to maximize the profits of the DSO, CSOs, and EVs. To highlight the contributions of this paper, Table 1 summarizes and compares the proposed EV charging station management methods with existing relevant literature. The contributions of this paper are threefold:

- 1) A resource allocation model is established among the DSO, CSOs, and EVs. The aggregate feasible power regions of CSOs are obtained based on a novel method with the combination of a model-based and data-driven scheme, which, along with distribution network clearing and EV demand response, collectively participate in the energy management of CSOs.
- 2) A hierarchical pricing mechanism for CSOs is proposed based on nodal clearing pricing and robust Stackelberg-based pricing. The DSO determines the distributed locational marginal prices (DLMP) according to the electricity market clearing mechanism to fairly distribute charging resources. CSOs formulate retail electricity prices based on their profits and the demand response profit of EV users.
- 3) A novel distributed management mechanism with a clear physical interpretation is designed to achieve distributed coordination of energy management among the DSO, CSOs, and EV users. It satisfies the privacy protection requirements of EV users while achieving optimal convergence and energy balance.

The rest of this paper is organized as follows: Section 2 briefly introduces the structure of the proposed two-stage energy management framework. In Section 3, the economic optimized models for the DSO, CSOs, and EV users are established, which include the demand response of EV users and aggregate feasible power regions of CSOs. Section 4 designs the hierarchical pricing mechanism of CSOs and establishes distributed energy management. Simulation verification and testing analysis are conducted in Section 5. Finally, conclusions are given at the end of the paper.

2. Two-stage energy management framework

A two-stage scheduling framework for the energy management of CSOs is constructed, as shown in Fig. 1. In the first stage, the optimization problem of this paper is modeled as a mixed-integer programming (MIP) problem, where the aggregate feasible power regions of CSOs obtained through the combination of Minkowski summation [15] and the data-driven method [31], the distribution network clearing mechanism, and the demand response of EV users are all considered. The objective function of the model reflects the economic profits of electricity purchase and sale for the DSO, CSOs, and EV users.

In the second stage, a hierarchical pricing mechanism is constructed to capture the relationships between the DSO and CSOs, as well as between CSOs and EV users. The electricity purchase and sale prices between the DSO and CSOs are determined by the DLMP. The retail electricity prices between CSOs and EV users are determined through a robust Stackelberg model. Finally, considering the privacy requirements of EV users, the hierarchical pricing mechanism and the coupling with the distribution network, a distributed coordination framework for the energy management of CSOs is established, which provides a transparent physical interpretation.

Table 1

Comparison of this paper with other related literature.

Ref.	Network Constraints	Distributed	EV users' DR	CSOs' Flexibility	Electrical Market	Clear Physical Interpretation
[11,12]	x	✓	x	x	x	✓
[13,14]	x	✓	✓	x	x	✓
[49,50]	x	✓	x	x	x	x
[16,18]	✓	x	x	x	x	x
[17]	✓	x	x	x	x	✓
[20,22,24,35]	✓	✓	x	x	x	x
[27,44]	✓	x	x	x	x	x
[30,32]	x	x	x	✓	x	x
[3,33]	✓	✓	✓	x	x	x
[26,34]	✓	✓	x	x	✓	✓
[28]	x	✓	✓	x	✓	x
[38,45,46]	x	x	✓	x	✓	x
[40,42]	✓	✓	x	x	✓	x
[3,43]	✓	✓	✓	✓	x	x
[47]	✓	✓	✓	x	✓	x
This paper	✓	✓	✓	✓	✓	✓

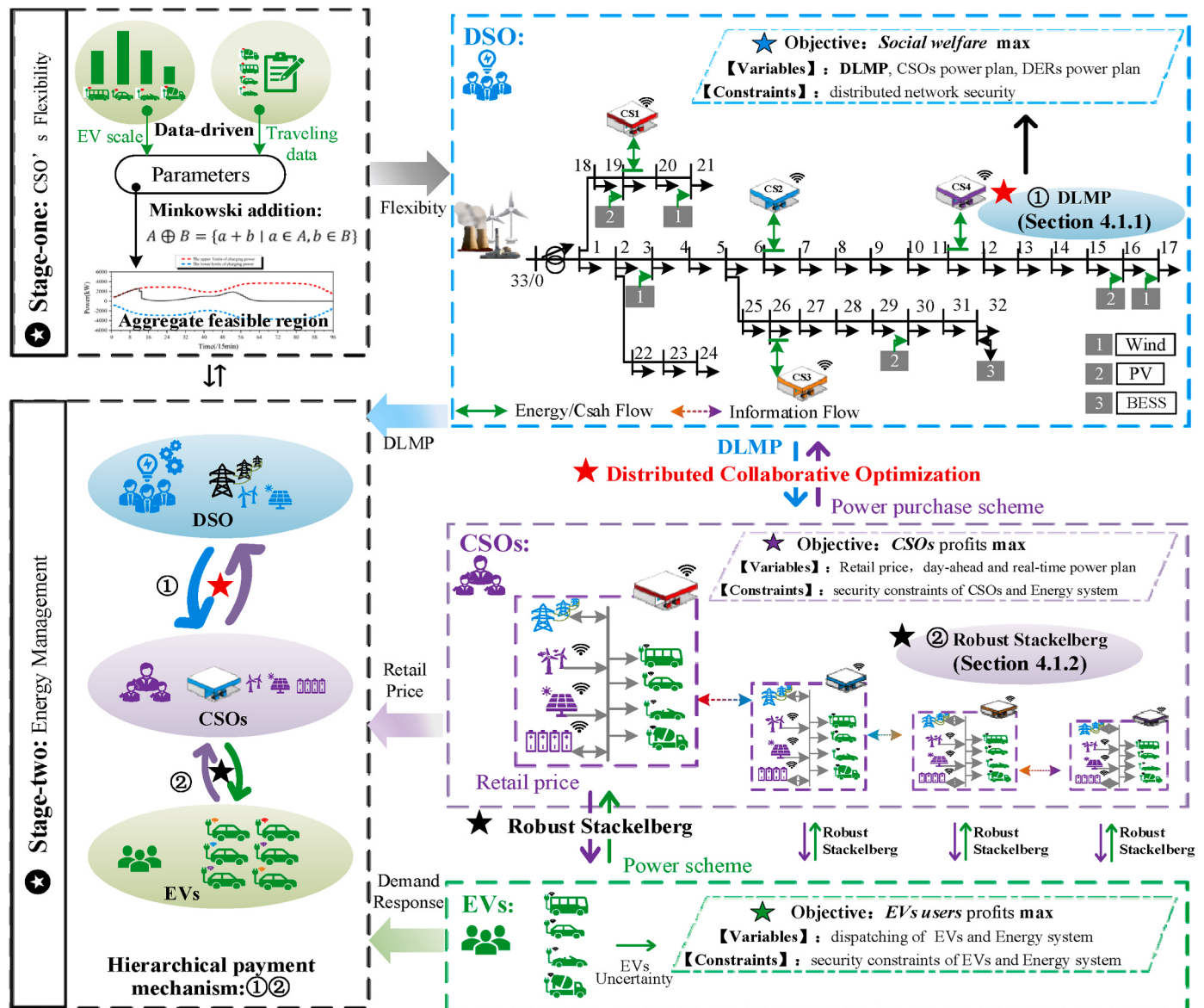


Fig. 1. Two-stage energy management framework of EV charging stations.

3. Stage-one: scheduling model of charging stations

In the first stage, it is necessary to integrate the optimization objectives of the DSO, CSOs, and EV users. As the upper-level grid operator, the DSO aims to achieve optimal power flow while satisfying network security constraints. On the other hand, CSOs need to develop reasonable retail pricing mechanisms and energy management strategies to participate in DSOs' bidding and auction processes in the day-ahead and real-time stages, maximizing their own economic benefits as well as the economic benefits of EV users. Therefore, this section models the objective functions of different participants separately.

3.1. Objective of the distribution system operator

Generally, the distribution network is modeled as a graph $G(N, E)$, where N and E represent the sets of buses and branches, respectively [51, 52]. To facilitate fast computation of large-scale distribution networks, the non-convex constraints of the distribution network power flow model are relaxed using second-order cone relaxation and polyhedral approximation techniques [53]. In [Appendix A.1](#), a dynamic optimal power flow model based on linearized second-order conic relaxation (LSOCR-OPF, [53]) for the DSO is established, which is easier to solve by invoking an advanced solver. The goal of the DSO is to minimize the total cost of social electricity consumption, whose objective function is shown as:

$$f_{DSO} = \underbrace{\sum_{t \in T} \sum_{jk \in \Omega} (\tilde{I}_{jk} r_{jk}) \lambda(t) \Delta t}_{f_{loss}} + \underbrace{\sum_{t \in T} (p_0^b(t) \gamma_{TSO}^b(t) - p_0^s(t) \gamma_{TSO}^s(t))}_{f_{TSO}} - \underbrace{\sum_{i \in N_{CSO}} (f_{CSO_i}^{Day-ahead} + f_{CSO_i}^{Real-time})}_{f_{CSO}} \quad (1)$$

where, λ embodies the price to turn the power loss into a monetary term. γ_{TSO}^b and γ_{TSO}^s are the utility (Transmission system operator, TSO) electricity buy and sale prices, respectively. $p_0^b(t)$ and $p_0^s(t)$ denote the energy bought/sold by bus 1 at time t . N_{CSO} represents the total number of CSOs. $f_{CSO_i}^{Day-ahead}$ and $f_{CSO_i}^{Real-time}$ are the day-ahead and real-time power plan cost of CSO_i , respectively. The cost of network loss is denoted as f_{loss} . The costs associated with the DSO procuring and selling electrical energy from/to the utility are denoted as f_{TSO} . r_{jk} is the resistance of branch jk . \tilde{I}_{jk} denotes the current flowing through branch jk at time t . $f_{g,i}$ represents the revenue obtained by the DSO from the purchasing plan of the CSO_i . Ω refers to the number of distribution network branches. T is the total number of time intervals.

It is evident that the optimal power flow model for DSOs fundamentally constitutes a mixed-integer programming problem [53]. In this paper, a radial distribution network is adopted with the value of K in [Appendix A.1](#) set to 11, which satisfies the accuracy requirements of both the second-order cone relaxation [54] and the polyhedral linearization approximation [55] of the objective of the DSO.

3.2. Objective of the charging station operators

The objective function of CSOs is to maximize profits during the bidding processes of the electricity clearing of the DSO in both the day-ahead and real-time stages. The decision variables include the day-ahead and real-time electricity purchases, the dispatch schedule of self-equipped distributed energy resources, and the retail electricity price of EVs. These variables need to satisfy constraints such as market trading rules, constraints of aggregate feasible regions, retail market pricing constraints, and energy balance constraints. In the day-ahead stage, CSOs need to decide on their purchased electricity amount and release their retail electricity price in the day-ahead electricity market to

maximize their own profits. In the real-time stage, CSOs will optimize their energy plan, including the charging and discharging of their battery energy storage system (BESS), renewable generation (Wind; Photovoltaic, PV), and the purchase and sale of electricity in the real-time electricity market based on the demand response of EV users (which will be analyzed in the next section), in order to minimize electricity purchase costs.

3.2.1. Aggregating feasible regions for charging stations

The aggregate feasible regions of CSOs are critical for their participation in the DSO's bidding and auction results. To quickly and accurately describe the aggregate feasible power regions of CSOs involving nonlinear variables, the idea of "Minkowski summation [56]" is borrowed in this study, and the CSO is regarded as a virtual energy storage device aggregated by EVs. The physical model of the individual EV is described in [Appendix A.2](#). Based on the Minkowski summation, the virtual energy storage device model of the CSO is obtained [15]:

$$\left\{ \begin{array}{l} 0 \leq P_{i,t}^{ch} \leq P_{i,t}^{ch,max}, \forall t \in T \\ 0 \leq P_{i,t}^{dis} \leq P_{i,t}^{dis,max}, \forall t \in T \\ S_{i,t} = S_{i,t-1} + \Delta S_{i,t} + \eta^{ch} P_{i,t}^{ch} \Delta t - \frac{\eta^{ref} P_{i,t}^{dis} \Delta t}{\eta^{dis}}, \forall t \in T \\ S_{i,t}^{min} \leq S_{i,t} \leq S_{i,t}^{max}, \forall t \in T \end{array} \right. \quad (2)$$

where, $P_{i,t}^{ch}$ and $P_{i,t}^{dis}$ denote the charging and discharging plan of CSO_i with the DSO at time t , respectively. $P_{i,t}^{ch,max}$ and $P_{i,t}^{dis,max}$ represent the maximum charging and discharging power of CSO_i at time t , respectively. $S_{i,t}$ denotes the energy level of CSO_i at time t , with $S_{i,t}^{max}$ and $S_{i,t}^{min}$ as its upper and lower limits. $\Delta S_{i,t}$ demonstrates the energy change of CSO_i caused by the connection/disconnection of EVs at time t . Δt is the duration of the change. η^{ch} and η^{dis} are the charging and discharging efficiencies, respectively. η^{ref} is the discharge replenishment coefficient, determined by the discharge loss. The parameters $\{P_{i,t}^{ch,max}, P_{i,t}^{dis,max}, \Delta S_{i,t}, S_{i,t}^{min}, S_{i,t}^{max}\}$ determine the aggregate feasible region of CSO_i as a virtual energy storage device.

Furthermore, the parameters of the equivalent virtual energy storage device for each charging station are computed based on the dataset in [Appendix B](#). The data-driven method in Ref. [31] is being used to achieve the classification and aggregation of large-scale EV. The historical EV data for each CSO is clustered into $n = 10$ classes, and the data is recorded as:

$$EV_n = \{T_n^{ar}, T_n^{de}, s_{n,ar}, s_{n,de}, S_n^{min}, S_n^{max}, P_{n,max}^{ch}, P_{n,max}^{dis}\} \quad (3)$$

where, T_n^{ar} represents the arrival time of EV_n at the charging station, while T_n^{de} stands for the departure time of EV_n . The variables $s_{n,ar}$ and $s_{n,de}$ denote the initial and expected battery levels of EV_n upon arrival and departure, respectively. Additionally, S_n^{max} and S_n^{min} indicate the upper and lower bounds of EV_n 's battery level, while $P_{n,max}^{ch}$ and $P_{n,max}^{dis}$ convey the maximum charging and discharging power limits of EV_n , respectively.

In the day-ahead stage, the parameters of each CSO as a virtual energy storage device are calculated by equation (2) based on the EV information from equation (3). These calculated parameters are then used to obtain the posteriori day-ahead aggregate feasible regions for CSOs, as shown:

$$\Pi_{CSO_i}^{Da} = \{P_{i,t}^{Da,ch,max}, P_{i,t}^{Da,dis,max}, \Delta S_{i,t}^{Da}, S_{i,t}^{Da,min}, S_{i,t}^{Da,max}\} \quad (4)$$

where, $\Pi_{CSO_i}^{Da}$ represents the day-ahead aggregate feasible region of CSO_i .

In the real-time stage, the CSOs calculate the real-time aggregate

feasible regions based on the measured data of EVs currently present at the charging station [57]. As shown in Fig. 2, the aggregate feasible power regions are continuously updated as time progresses, but only a rolling time window plan is executed during the scheduling process. The corresponding real-time aggregate feasible region is expressed as:

$$\Pi_{CSO_i}^{Re} = \left\{ P_{i,t}^{Re, ch, max}, P_{i,t}^{Re, dis, max}, \Delta S_{i,t}^{Re}, S_{i,t}^{Re, min}, S_{i,t}^{Re, max} \right\} \quad (5)$$

where, $\Pi_{CSO_i}^{Re}$ represents the real-time aggregate feasible region of CSO_i .

The complete procedure for obtaining the aggregate feasible regions of CSOs is as follows: 1) Based on the collected EV information and the behavior characteristics distribution of EV users, a Monte Carlo sampling method is employed to generate eight feature parameter ranges, including the initial state of charge (SOC) of EVs. 2) Using the EVs information generated from the Monte Carlo sampling, the complete behavioral boundaries of the EVs are determined. 3) The overall behavioral boundaries of each type of EV are aggregated through Minkowski summation, and the total power boundaries and energy boundaries for the day-ahead and real-time stages are derived based on equation (2). These boundaries are used for energy management during the first stage. It is assumed that EV users prefer to reserve charging stations in advance by submitting parameters one day ahead [7]. For EV users, reserving charging stations allows them to reduce charging waiting time and potentially generate income through flexible charging and discharging using vehicle-to-grid (V2G) technology [58].

3.2.2. Model of the charging station operators

Based on the outcomes of the day-ahead and real-time aggregate feasible power regions of CSOs, in the day-ahead stage, CSOs need to make decisions on the amount of electricity they purchase from the day-ahead power market and publish their retail electricity prices to maximize their profits. In the real-time stage, CSOs will optimize the electric energy plan according to the actual EV charging and discharging capacity, including the charging and discharging capacity of the BESS and the purchase and sale of energy from the real-time power market. The uncertainty of EV users is considered in this section, and a robust Stackelberg model is developed to calculate the power schedule of CSOs and profits under the worst-case scenario. The objective function comprises the profit from day-ahead power purchases and the expected income from real-time operations, which is described by:

$$f_{CSO_i} = \max \left\{ \Pi_{CSO_i}^{Da}, \Pi_{CSO_i}^{Re} \right\} = \max \left\{ - \sum_{t \in T} \left(\mu_{i,t}^{Da} P_{b,i,t}^{Da} \right) + \right. \right.$$

$$\left. \left. - f_{CSO_i}^{Day-ahead} \right\}$$

$$\min \max_{\{\mathcal{N}^{EV} \in \mathbb{E}(DR_n^{EV})\}} \left\{ \underbrace{\sum_{t \in T} \sum_{n \in \mathcal{N}^{EV}} \left(\pi_t p_{ch,n,t}^{EV} - \pi_t p_{dis,n,t}^{EV} \right)}_{f_{EVs}^{cost}} + \underbrace{\sum_{t \in T} \left(\mu_{i,t}^{Re} P_{s,i,t}^{Re} - \mu_{i,t}^{Re} P_{b,i,t}^{Re} \right)}_{-f_{CSO_i}^{Real-time}} \right\} \quad (6a)$$

$$\text{s.t. } -P_{b,i,t}^{Da, dis, max} \leq P_{b,i,t}^{Da} \leq P_{b,i,t}^{Da, ch, max}, \forall t \in T, \forall i \in N_{CSO} \quad (6b)$$

$$\begin{cases} 0 \leq P_{b,i,t}^{Re} \leq P_{i,t}^{Re, ch, max}, \forall t \in T, \forall i \in N_{CSO} \\ 0 \leq P_{s,i,t}^{Re} \leq P_{i,t}^{Re, dis, max}, \forall t \in T, \forall i \in N_{CSO} \end{cases} \quad (6c)$$

$$\mu_{i,t}^{Da} = \varphi_t \left(P_{b,i,t}^{Da} \right), \forall t \in T, \forall i \in N_{CSO} \quad (6d)$$

$$\begin{aligned} P_{b,i,t}^{Da} + P_{b,i,t}^{Re} + P_{pv,i,t} + P_{wind,i,t} + P_{dis,i,t}^{BESS} + \sum_{n \in \mathcal{N}^{EV}} p_{dis,n,t}^{EV} \\ = P_{s,i,t}^{Re} + P_{ch,i,t}^{BESS} + \sum_{n \in \mathcal{N}^{EV}} p_{ch,n,t}^{EV}, \forall t \in T, \forall i \in N_{CSO} \end{aligned} \quad (6e)$$

$$E_n = \arg \max \mathbb{E}(DR_n^{EV}), \forall t \in T \quad (6f)$$

where, $\mu_{i,t}^{Da}$ and $\mu_{i,t}^{Re}$ represent the day-ahead and real-time clearing price of CSO_i (DLMP, [59]) at time t , respectively. $P_{b,i,t}^{Da}$, $P_{s,i,t}^{Re}$ and $P_{b,i,t}^{Re}$ embody the day-ahead and real-time energy plan of CSO_i at time t , respectively. π_t denotes the retail electricity price at time t . \mathcal{N}^{EV} represents the set of electric vehicle types, which includes N_{type} elements. $\mathbb{E}(DR_n^{EV})$ represents the expected value of EV users' demand response profits. A Stackelberg game is formed between the CSO and EV users due to conflicting decision order and interests (DR_n^{EV}). $P_{ch,i,t}^{BESS}$ and $P_{dis,i,t}^{BESS}$ denote the power schedule of the BESS equipped by CSO_i at time t . $P_{wind,i,t}$ and $P_{pv,i,t}$ refer to the power generation of wind and PV equipped with CSO_i at time t . $p_{ch,n,t}^{EV}$ and $p_{dis,n,t}^{EV}$ represent the charge and discharge plan of EV_n at time t , which is determined by demand response profits function of EV users (Equation (7)). f_{EVs}^{cost} refer to the charging and discharging cost of EVs participating in demand response.

Equation (6b) restricts the day-ahead power purchases of CSOs. However, in practice, selling electricity to the DSO will not be conducted by CSOs in the day-ahead stage. Equation (6c) represents the restriction of CSOs' real-time purchase and sale power. The day-ahead and real-time electricity trading behaviors of the CSOs are constrained by the aggregate feasible regions. Equation (6d) conveys the DLMP at the CSOs' node, which is fitted as a linear function of the variable $\{P_{b,i,t}^{Da}\}$. Equation (6e) indicates the balance of active power. Equation (6f) denotes the demand response of EV users as the lower-level follower in the robust Stackelberg model. The additional constraints and explanations of equation (6) can be found in Appendix A.3.

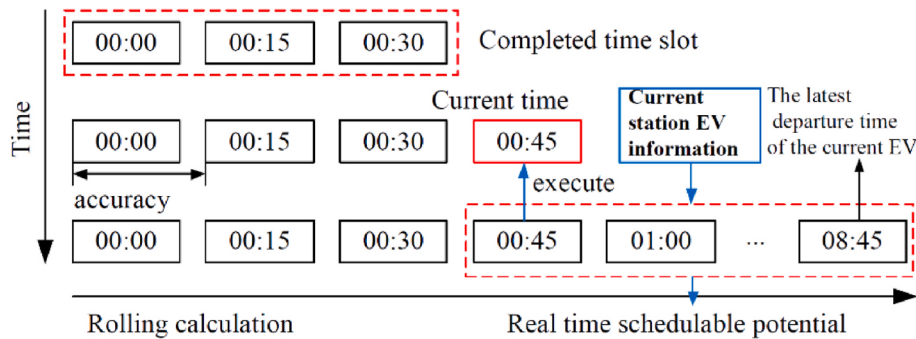


Fig. 2. Real-time schedulable potential.

3.3. Objective of the electric vehicles

The scheduling plan of EV users is only reflected in the real-time stage. The EV users determine their charging and discharging behavior based on the retail electricity prices published by CSOs. The objective of EV users is to maximize their utility through demand response:

$$f_{EV_s} = \max_{p_{ch,n,t}^{EV}, p_{dis,n,t}^{EV}, s_{n,t}^{EV}, \pi_t, n \in \mathcal{N}^{EV}} \mathbb{E}(DR_n^{EV}) = \sum_{t \in T} \left[\underbrace{\alpha_{n,t}^{EV} \left(\eta_{ch}^{EV} p_{ch,n,t}^{EV} - \frac{p_{dis,n,t}^{EV}}{\eta_{dis}^{EV}} \right)}_{f_{EV_s}^{utility}} - \underbrace{\pi_t (p_{ch,n,t}^{EV} - p_{dis,n,t}^{EV})}_{f_{EV_s}^{cost}} \right] \quad (7)$$

where, $s_{n,t}^{EV}$ denotes the amount of electricity consumed by EV_n at time t . η_{ch}^{EV} and η_{dis}^{EV} convey the charging and discharging efficiencies of EVs, and $\alpha_{n,t}^{EV}$ defines the unit utility of EV_n at time t . $\mathbb{E}(\cdot)$ is the expected value of EV users' profits. The utility function for EVs participating in demand response is represented by $f_{EV_s}^{utility}$.

The constraints and explanations of equation (7) can be found in [Appendix A.4](#). The electricity consumption behavior of EV users is determined by the retail electricity prices set by CSOs. However, the actual preferences for EV behavior are uncertain and cannot be predicted in advance. Therefore, the pricing decisions of CSOs need to consider the uncertainty of EVs. Building upon the principle of distributed robust optimization, a substantial amount of historical EV data is grouped into \mathcal{N}^{EV} clusters, considering the uncertainties associated with the probabilities of each type of EV. Given that the actual distribution might be different from this empirical distribution, a confidence set for the ambiguous distribution is constructed. Two norms are used to construct two types of confidence sets. This allows the charging and discharging profiles of the EV clusters to be described as [\[60\]](#):

$$\begin{cases} \sum_{n \in \mathcal{N}^{EV}} p_{ch,n,t}^{EV} \triangleq N_{EV} \sum_{n \in \mathcal{N}^{EV}} \sigma_n p_{ch,n,t}^{EV}, \forall t \in T, \forall n \in N_{EV} \\ \sum_{n \in \mathcal{N}^{EV}} p_{dis,n,t}^{EV} \triangleq N_{EV} \sum_{n \in \mathcal{N}^{EV}} \sigma_n p_{dis,n,t}^{EV}, \forall t \in T, \forall n \in N_{EV} \end{cases} \quad (8a)$$

$$p_{ch,n,t}^{EV} \bullet p_{dis,n,t}^{EV} = 0, \forall t \in T, \forall n \in N_{EV} \quad (8b)$$

$$\mathcal{R} = \begin{cases} \|\sigma - \sigma_0\|_1 \leq \theta_1 \\ \|\sigma - \sigma_0\|_\infty \leq \theta_\infty, \sigma \in \mathbb{R}_{N_{type}} \\ \|\sigma\|_1 = 1 \end{cases} \quad (8c)$$

where, \mathcal{R} represents an uncertain set, σ is a vector composed of the distribution of uncertain variables, i. e $\sigma = \{\sigma_n, \forall n \in \mathcal{N}^{EV}\}$, which denotes the proportion of EV_n . σ_0 is the original distribution of uncertain variables. The average number of EVs served by the CSO in one day is N_{EV} . θ conveys the corresponding tolerance value of \mathcal{R} , derived from the given confidence level and the amount of historical data. Equation (8a) details the charging and discharging capacity of EV clusters. The charging and discharging constraints of EVs are expressed by equation (8b). The uncertain space constituted by the proportional composition of different types of EVs is represented by equation (8c).

4. Stage-two: Distributed energy management of charging stations

The benefits of the DSO, CSOs, and EV users are interconnected through the proposed pricing mechanism. In the second stage, to maximize the expected profits of all three parties, a hierarchical pricing

mechanism based on price-driven models is designed for the intermediary CSOs. A robust Stackelberg model is established based on the objective functions of CSOs and EV users in [Sections 3.2.2](#) and [3.3](#), respectively. Moreover, considering the uncertainties and privacy requirements of EV users, an energy management mechanism based on distributed coordinated optimization is established between the DSO and CSOs.

4.1. Hierarchical pricing mechanisms of charging station operators

The DSO determines the purchase and sale prices between different CSOs under different node positions through the electricity market clearing model, and CSOs establish economic connections with EV users by setting retail electricity prices. The proposed hierarchical pricing mechanism includes two levels of pricing strategies, which reflect the active participation of CSOs in energy management and the demand response of EV users, respectively.

4.1.1. Clearing price strategy between the distributed network and charging stations

In the first level pricing mechanism, to reflect the CSO's active participation in DSO's energy management, let i be the bus node of the DSO at the location of CSO $_i$ and the power balance at node i is shown as:

$$\begin{cases} P_{b,i,t}^{Da} = p_{jk,i,t}^{Da} : \mu_{p,i,t}^{Da} \\ P_{s,i,t}^{Re} - P_{b,i,t}^{Re} = p_{jk,i,t}^{Re} : \mu_{p,i,t}^{Re} \end{cases} \quad (9)$$

where, $\mu_{p,i,t}^{Da}$ and $\mu_{p,i,t}^{Re}$ denote the dual variables of the corresponding constraints and represent the DLMP at the CSO's location. Here, the dual variable corresponding to the constraint is represented by a colon [\[61\]](#). $p_{jk,i,t}^{Da}$ and $p_{jk,i,t}^{Re}$ are the day-ahead and real-time active power flow of the DSO in branch jk .

The day-ahead and real-time electricity prices $\{\mu_{p,i,t}^{Da}, \mu_{p,i,t}^{Re}\}$ are determined by market clearing and are influenced by the energy plan of CSOs. In the retail electricity market, the EVs aggregated by the CSO submit the bid according to the step function. When there are enough CSOs, a linear function can accurately fit the market clearing curve. As shown in [Fig. 3](#), when CSOs buy electricity from the DSO, the clearing price increases with the increase in load according to the law of increasing marginal cost, and vice versa.

Regarding the bilinear terms $\{\mu_{p,i,t}^{Da} p_{b,i,t}^{Da}, \mu_{p,i,t}^{Re} p_{b,i,t}^{Re}, \mu_{p,i,t}^{Re} p_{s,i,t}^{Re}\}$ in equation (6a), a general solution method has been proposed in [Ref. \[62\]](#). Considering the difficulty in solving the Karush-Kuhn-Tucker conditions of the electricity market clearing model and the strict mapping relationship between the power transactions of CSOs and DLMP (as illustrated in [Fig. 4](#), the DLMP at a fixed time is roughly proportional to the purchased power), this study adopts a method of incrementally

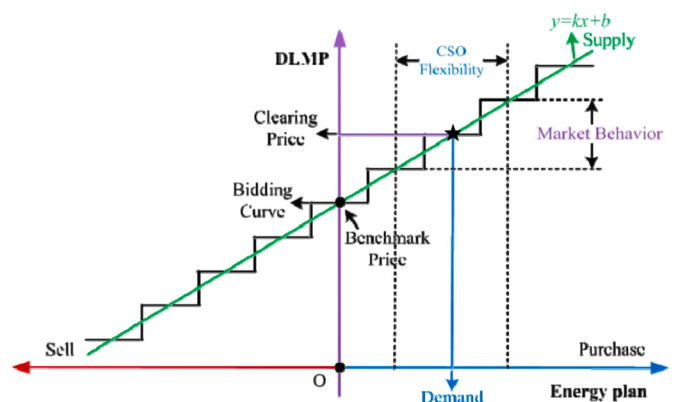


Fig. 3. Forecast curve of market clearing price.

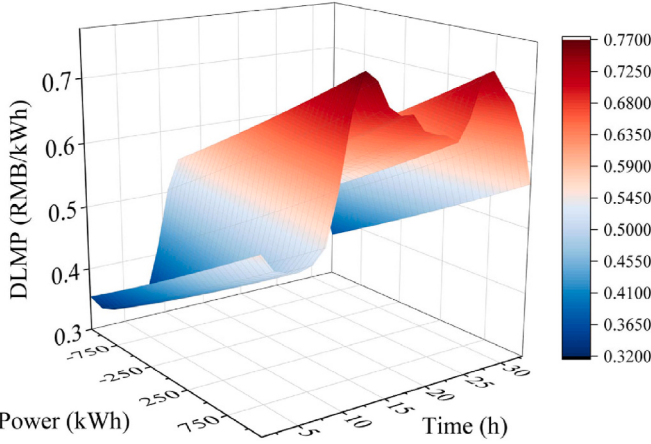


Fig. 4. Relationship between node 6's DLMP and CSO₂'s power.

increasing the active power at the electrical nodes where CSOs are located. Multiple iterations of AC power flow models are solved to obtain the dual variables. Subsequently, a market clearing function for DLMP and the electricity purchases of CSOs is fitted using the least squares method. The clearing price can be predicted by the DSO and CSOs through:

$$\begin{cases} \mu_{p,i,t}^{Da} = \alpha_t^{Da} P_{b,i,t}^{Da} + \beta_t^{Da} \\ \mu_{p,i,t}^{Re} = \alpha_t^{Re} (P_{b,i,t}^{Re} - P_{s,i,t}^{Re}) + \beta_t^{Re} \end{cases} \quad (10)$$

where, α_t^{Da} and α_t^{Re} represent the sensitivity coefficient of the day-ahead and real-time electricity price at time t , respectively. β_t^{Da} and β_t^{Re}

represent the day-ahead and real-time base price at time t , respectively. the coefficients α_t^* and β_t^* in the equation are obtained by the least-squares method. Hence, the bilinear terms $\{\mu_{p,i,t}^{Da} P_{b,i,t}^{Da}, \mu_{p,i,t}^{Re} P_{b,i,t}^{Re}, \mu_{p,i,t}^{Re} P_{s,i,t}^{Re}\}$ can be converted to quadratic function.

4.1.2. Retail pricing strategy between charging stations and electric vehicles

In the second-level pricing strategy, to capture the demand response of EVs, a two-stage robust retail pricing strategy is developed for CSOs, as presented in equations (6) and (7) in Sections 3.2.2 and 3.3. The objective of the robust pricing strategy is to maximize the benefits for both CSOs and EV users. The decision variables encompass retail electricity prices, as well as the electricity consumption plans of CSOs and EVs, while satisfying the constraints imposed by market trading rules, retail market pricing, and energy balance. Within this process, the EV demand response model (denoted as f_{EV_s}) serves as a follower in the Stackelberg model (f_{CSO_i}), describing the mapping between retail electricity prices and EVs energy plans. equations (6) and (7) constitute a typical two-stage robust optimal problem based on Stackelberg and can be solved through column-and-constraint generation (CC&G, [19]), Karush-Kuhn-Tucker, and strong duality. The flowchart for solving the above model by CC&G is shown in Fig. 5.

4.2. Distributed coordination mechanism

Based on the aforementioned model, the power exchange between CSOs and the DSO is facilitated through equation (9). Following equivalent transformations detailed in Appendix A.5, a framework is presented that adopts the classical distributed ADMM optimization algorithm to solve the distributed optimization of the DSO, CSOs and EVs. It has been proven that the distributed ADMM framework exhibits good convergence performance and can converge to a centralized optimum if

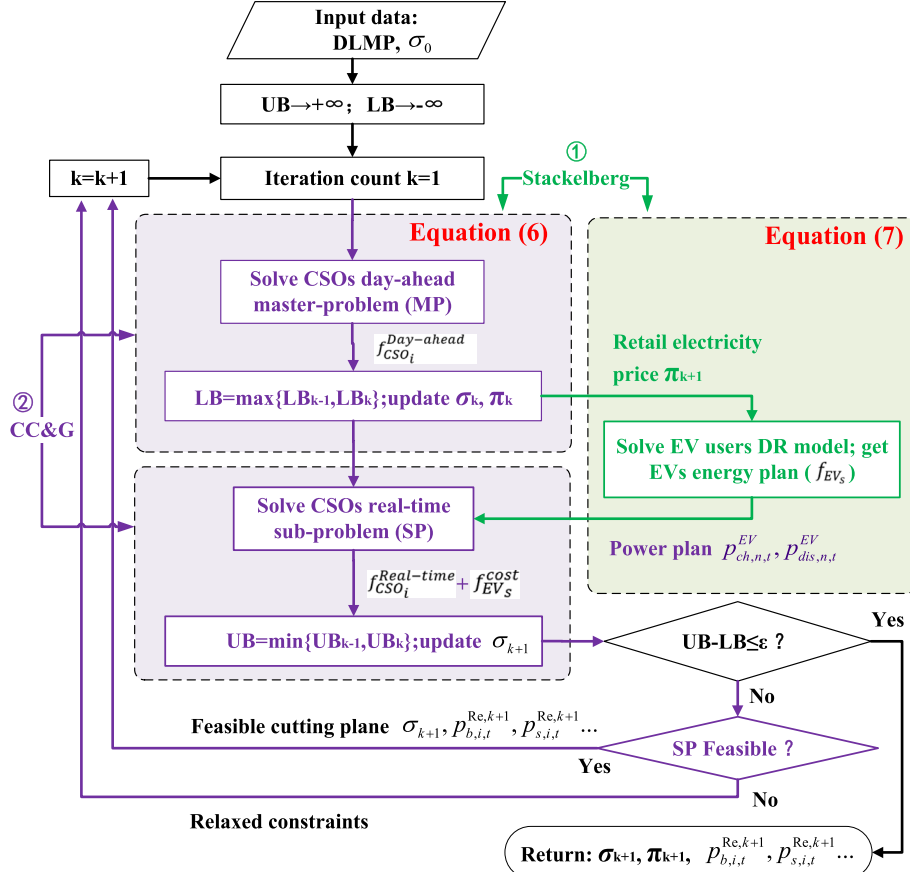


Fig. 5. Flowchart of the proposed two-stage robust Stackelberg pricing strategy of CSOs.

the problem is convex [26]. The coordination mechanism operates in an iterative process. In the $(k+1)_{th}$ iteration:

The objective function of CSO_i is changed to:

$$f_{CSO_i} = \underbrace{\max \left\{ f_{CSO_i}^{Day-ahead} \right\} + \min_{\{i' \in \mathbb{E} \in \mathbb{E}(DR_n^{EV})\}} \left\{ f_{EV_s}^{cost} + f_{CSO_i}^{Real-time} \right\}}_{f_{CSO_i}} + \sum_{t \in T} \frac{\rho}{2} \left\| \underbrace{P_{b,i,t}^{Da} + (P_{s,i,t}^{Re} - P_{b,i,t}^{Re})}_{p_{g,i,t}^{k+1}} - \underbrace{(P_{jk,i,t}^{Re} + p_{jk,i,t}^{Da})}_{p_{jk,i,t}^{k+1}} \right\|_2 \quad (11a)$$

$$\text{s.t.} \begin{cases} (1), (2), (\text{Appendix A.2} \sim \text{A.3}) \\ \begin{cases} f_{EV_s} = \max \mathbb{E}(DR_n^{EV}) \\ \text{s.t.} \quad (\text{Appendix A.4}) \end{cases} \end{cases} \quad (11b)$$

where, $p_{jk,i,t}^k$ and $\mu_{p,i,t}^k$ are the given desired energy schedule and energy trading prices announced by the DSO, respectively. The last 2-norm term in equation (11a) represents the gap between the actual energy trading profile of CSO_i ($p_{g,i,t}^{k+1}$) and the schedule of the DSO. The CSO_i needs to meet schedule of the DSO as much as possible. The optimal energy trading profile of CSO_i is defined as $p_{g,i,t}^{k+1}$. ρ is the penalty parameter.

The objective function of the DSO is changed to:

$$f_{DSO} = f_{loss} + f_{TSO} + \sum_{i \in N_{CSO}} (f_{CSO_i}) + \sum_{t \in T} \frac{\rho}{2} \left\| p_{g,i,t}^{k+1} - p_{jk,i,t}^{k+1} \right\|_2 \quad (12a)$$

$$\text{s.t. LSOCR} - \text{OPF}(\text{Appendix A.1}), (9) \quad (12b)$$

where, $p_{g,i,t}^{k+1}$ is the desired energy trading profiles submitted by CSO_i . The DSO will adjust the energy plan ($p_{jk,i,t}^{k+1}$) to meet the needs of CSO_i . The 2-norm term in equation (12a) carries the same meaning with equation (11a) for the $(k+1)_{th}$ iteration. Equations (11) and (12) together constitute the distributed coordination among the DSO, CSOs, and EV users.

Algorithm 1 provides a comprehensive description of the proposed distributed coordination energy management in this study. The data that exchanged between CSOs and the DSO mainly includes energy trading plans and transaction prices. Therefore, the private data of each CSO and the network parameters owned by the DSO can be protected under the proposed distributed algorithm optimization, with a clear physical mechanism explanation. During the k_{th} iteration, CSO_i updates its own energy plan $\{p_{g,i,t}^{k+1}\}$ based on the energy transaction plan $\{p_{jk,i,t}^k\}$ and energy transaction prices $\{\mu_{p,i,t}^k\}$ announced by the DSO. In the $(k+1)_{th}$

iteration, the DSO updates the energy dispatch plan $\{p_{jk,i,t}^{k+1}\}$ based on the expected energy plan $\{p_{g,i,t}^{k+1}\}$ of CSO_i . Simultaneously, the energy transaction prices (DLMPs) are updated as $\{\mu_{p,i,t}^{k+1} = \mu_{p,i,t}^k + \rho(p_{g,i,t}^{k+1} - p_{jk,i,t}^{k+1})\}$, where the trend of DLMP changes is consistent with the market clearing model shown in Fig. 3. The convergence criterion for iteration is given by $\{\|\mu_{p,i,t}^{k+1} - \mu_{p,i,t}^k\| \leq \varepsilon\}$.

Based on the modeling process described above, the solution process diagram for the proposed distributed energy management framework of CSOs under the aggregate feasible power regions of CSOs and hierarchical pricing mechanism is illustrated in Fig. 6. The ADMM-based distributed optimization solution employed in this study ensures the effective protection of privacy for CSOs and the information of EV users within their coverage areas. It should be noted that the nonlinearity of the complementary constraints in CSO's energy storage charge and discharge, real-time power purchase and sale, and EV charge and discharge increases the computational difficulty of model solving. All complementary constraints presented in this paper have been proven to be redundant, as detailed in Appendix C. For the nonconvex constraint in equation (1), convex relaxation is performed to turn it into a second-order conic inequality constraint. The exactness of relaxation has been verified for the radial distribution network [19]. After the equivalent transformations in Appendix A.5, the proposed mechanism turns into the classical ADMM framework. Moreover, the focus of this paper is on flexible loads in power systems, such as EVs in distribution networks. The model relies on advanced communication systems to support coordination among DERs, CSOs, and the DSO. The development of intelligent meters and communication technologies provides a technical foundation for communication systems [63].

5. Simulations and discussions

In this section, the proposed approach is validated using an enhanced IEEE 33-test system [64] and four charging stations, including the aggregate feasible power regions of CSOs and the hierarchical pricing mechanism, as well as the distributed coordination and energy management mechanisms among the DSO, CSOs, and EVs. The simulation is performed on a 64-bit Windows 11 operating system with an Intel(R) Core (TM) i7-6700HQ CPU @ 2.64 GHz and 24 GB RAM, using MATLAB R2022b and calling YALMIP and GUROBI 10.0 [65].

5.1. System parameter settings

A distribution system with four charging stations is considered in this study. The four CSOs are located at nodes 19, 26, 6, and 27 of the IEEE 33 distribution system. The voltage upper and lower limits for each bus in the distribution network are set at 1.05 p. u. and 0.95 p. u., respec-

Algorithm 1 Distributed Coordination Mechanism.

Input: iteration index $k = 0$, convergence error tolerance $\varepsilon > 0$, penalty parameter $\rho > 0$, charging stations $i \in N_{CSO}$, aggregate feasible region of CSO_i , Π .

Output: trading price $\mu_{p,i,t}^{k+1}$, desired traded energy $p_{g,i,t}^{k+1}/p_{jk,i,t}^{k+1}$

- 1: **repeat**
- 2: **CSOs :**
- 3: **for** CSO_i **do** solve Equation (11) and report $p_{g,i,t}^{k+1}$ to DSO
- 4: **end for**
- 5: **DSO :**
- 6: **for** DSO **do** solve Equation (12) and report $p_{jk,i,t}^{k+1}$ to CSO_i
- 7: **end for**
- 8: **while** $\|\mu_{p,i,t}^{k+1} - \mu_{p,i,t}^k\| > \varepsilon$ **do** $\mu_{p,i,t}^{k+1} = \mu_{p,i,t}^k + \rho(p_{g,i,t}^{k+1} - p_{jk,i,t}^{k+1})$, $k = k + 1$
- 9: **end while**
- 10: **until** meet the convergence stopping criterion.

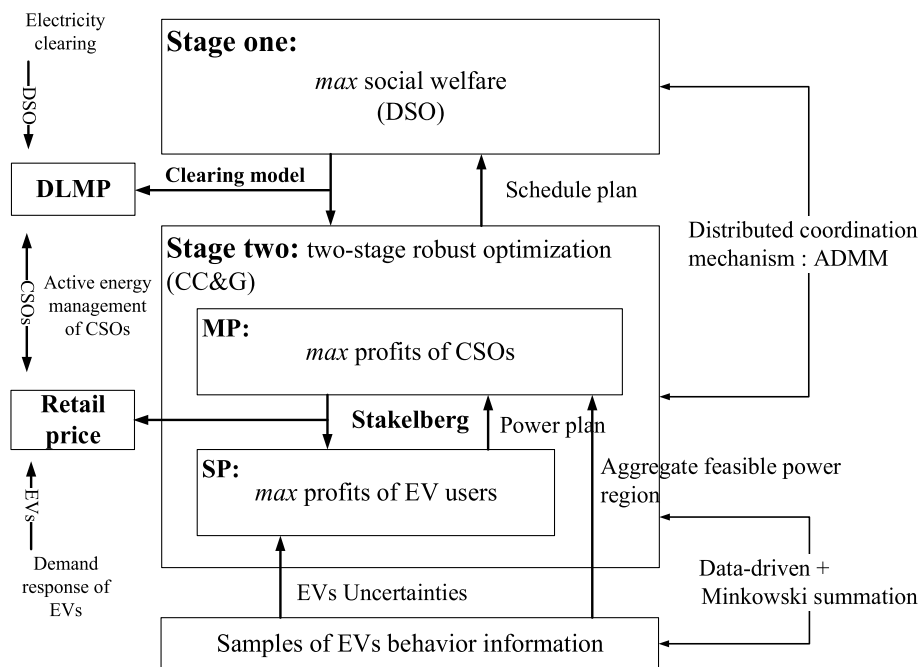


Fig. 6. Flowchart of the proposed methodology.

tively. This study randomly sampled 1000 EV data points from each of the four charging stations and categorized the data points into 10 groups. The characteristics of the 10 types of EVs within the coverage area of CSO_1 are presented in Table 2. The clustering results for the other three charging stations can be found in Appendix B. The charging/discharging efficiency of EVs is 0.95. The unit utility of EVs remains constant at 1 RMB/kWh. The BESS equipped by each CSO has a capacity of 2000 kWh, and the maximum charging and discharging power is 500 kW. The efficiency of the BESS for charging and discharging is 0.95, and the safe range for its SOC is set between 20 % and 95 %. The maximum real-time electricity purchase/sale quantity is 1000 kWh, and the maximum day-ahead electricity purchase quantity of every CSO is set to 1000 kWh. Each CSO is equipped with a PV unit with an installed capacity of 150 kW and a wind unit with an installed capacity of 120 kW. The capacity parameters for the wind unit, PV generation, and BESS are based on similar typical parameters in Ref. [66]. The real data for PV and

wind power generation are obtained from NREL [67]. More detailed simulation parameters can be found in Appendix B.

5.2. Simulation results and discussions

In order to evaluate the performance of the proposed distributed energy management of CSOs, some practical issues related to the proposed framework are discussed in this part [68]. Firstly, a comparison is conducted between existing EV aggregate feasible power region prediction methods and the proposed combining Minkowski summation with the data-driven method. The reliability of the solution results under relaxation techniques was also tested. Secondly, the proposed hierarchical pricing mechanism is compared through experimental studies with two common economic modes: price-taker mode and centralized scheduling mode. Additionally, characteristics of different electricity trading prices of CSOs, sensitivity analysis of uncertainties in large-scale EVs, and the impact of EV utility functions on demand response are analyzed. Finally, an analysis of the application potential and promotion value of the proposed energy management framework is provided.

Table 2
Parameters of different types of electric vehicles in CSO_1 .

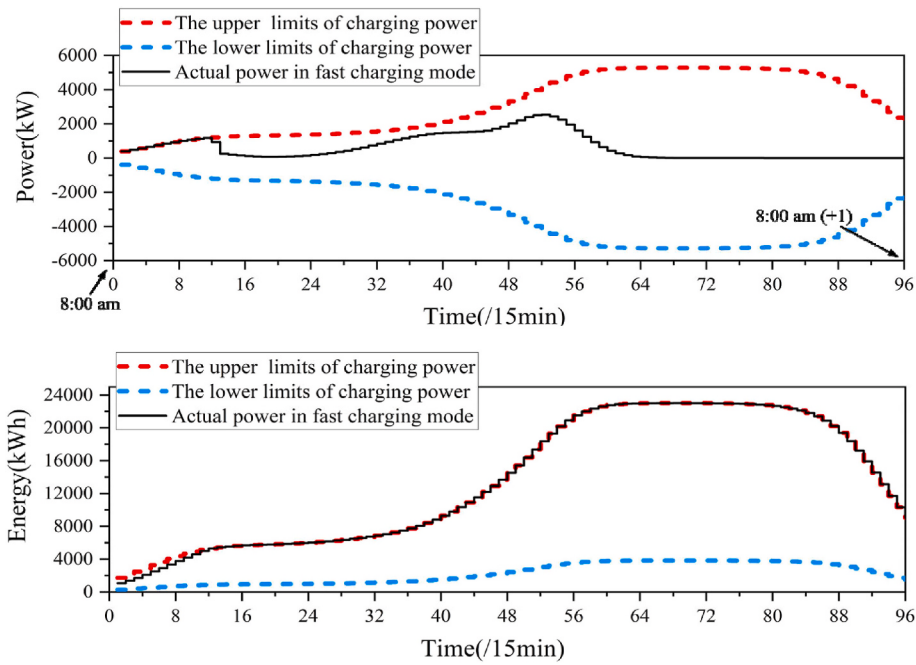
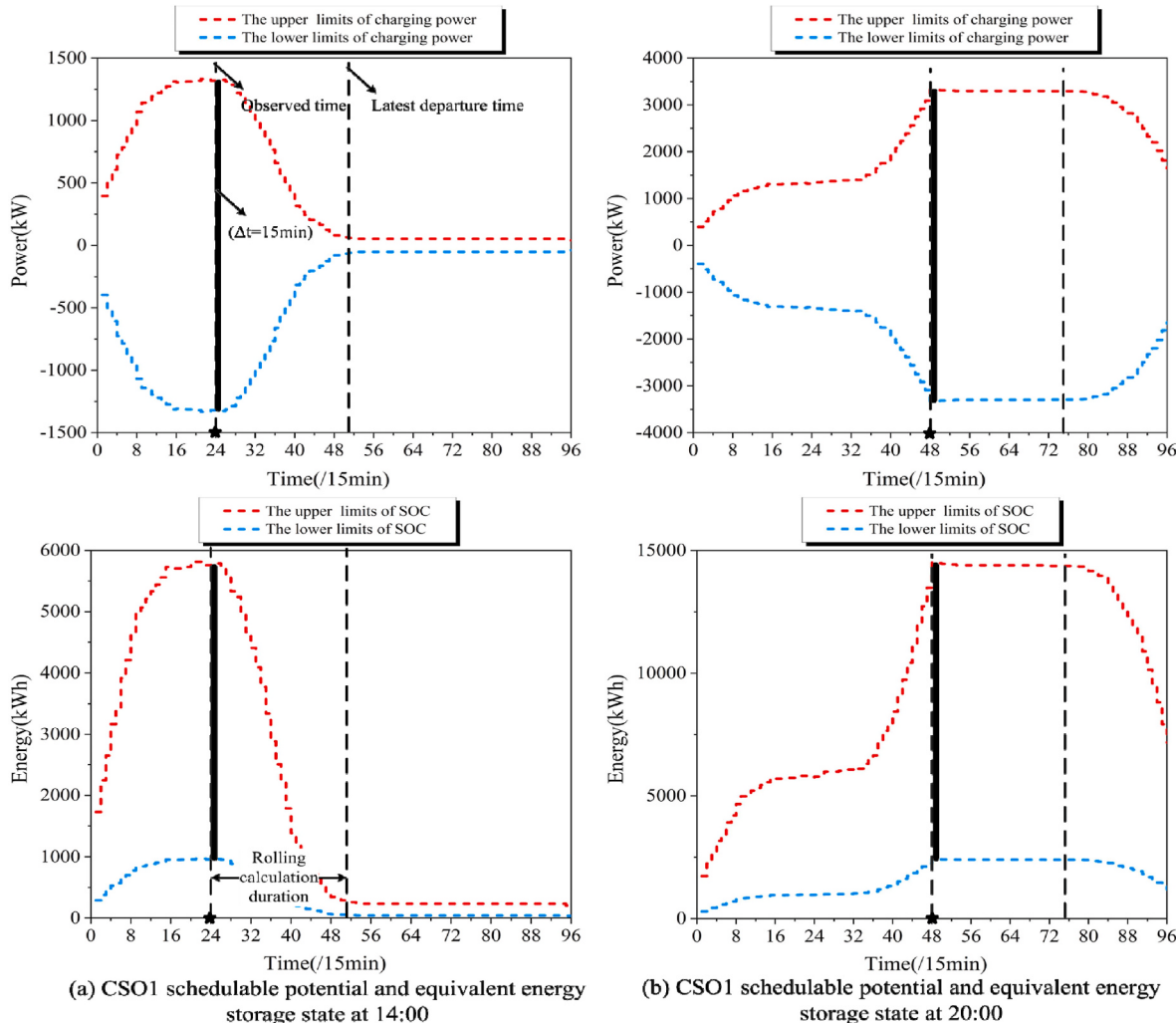
EV _n	Maximum power (kW)	Battery capacity (kWh)	Original power (kWh)	Arrive	Leave	Frequency
EV ₁	6	35	15	17:00	08:00 (+1)	105
EV ₂	8	32	16	09:00	17:00	52
EV ₃	4	30	10	18:00	07:00 (+1)	90
EV ₄	6	24	12	21:00	06:00 (+1)	157
EV ₅	6	43	25	08:00	16:00	80
EV ₆	8	45	16	19:00	07:00 (+1)	95
EV ₇	3	24	8	17:00	08:00 (+1)	135
EV ₈	12	45	20	09:00	17:00	68
EV ₉	10	40	18	18:00	08:00 (+1)	112
EV ₁₀	10	64	25	18:00	07:00 (+1)	106

Notes: Commuter group: EV₂, EV₅, and EV₈; private car group: EV₁, EV₃, EV₇, EV₉, and EV₁₀; ride-hailing group: EV₄ and EV₆.

5.2.1. Aggregate feasible regions of charging stations

By analyzing a dataset of 1000 historical data points, evaluation values for the aggregate feasible region of each CSO are obtained. Taking CSO_1 as an example, its day-ahead aggregate feasible region is depicted in Fig. 7. The proposed aggregate feasible region represents a collection of constraints on the charging and discharging power and SOC of the EV cluster, which encapsulate all possible charging and discharging decisions. The power curve of charging, as exemplified in Fig. 7, represents specific instances within this enveloping space. By considering CSOs as virtual energy storage devices, the aggregation of EVs is achieved. In comparison to actual energy storage devices, charging stations act as virtual energy storage devices with variable capacity, which is determined by the docking characteristics of EVs. The day-ahead aggregate feasible regions of the other three CSOs can be found in Appendix D.

The real-time aggregate feasible region is computed based on the real-time observed EV data within the charging station. Similarly, taking CSO_1 as an example, its real-time aggregate feasible region is illustrated in Fig. 8. As the charging station cannot predict future EV data, the real-

Fig. 7. Day-ahead aggregate feasible region of CSO₁.Fig. 8. Real-time aggregate feasible region of CSO₁.

time aggregate feasible region relies on the observed data in the current time period and is continuously updated as time progresses, as shown in Fig. 8. The real-time aggregate feasible regions of the four CSOs at different time periods can be found in Appendix D.

The deviation between the real-time aggregate feasible region and the day-ahead aggregate feasible region is depicted in Fig. 9. This deviation indicates that, on one hand, the day-ahead and real-time aggregate feasible regions exhibit similar shapes. This similarity can be attributed to the tidal effect of EV travel behavior and the ability of individual EV differences to offset each other, resulting in certain regularities observed in the EV cluster. On the other hand, it also highlights the existence of discrepancies between the day-ahead and the real-time aggregate feasible power regions. Therefore, it is imperative to utilize the real-time market to mitigate power deviations and ensure the power balance of the charging stations.

To verify the advantages of the proposed aggregate feasible power region calculation method for CSOs, we further compared its impact on optimization results with different dispatchable potential prediction methods. Specifically, the authors of [30] accurately modeled the dispatchable area of electric vehicles. Although the authors of [16] modeled an electric vehicle cluster, they did not consider energy boundary constraints. The authors of [31,32] constructed EV cluster models using big data analysis and data-driven methods, respectively. In contrast, this paper establishes a generalized energy storage model for charging stations based on Minkowski summation. Historical data was used to predict generalized energy storage device parameters through a data-driven method. The comparison results are presented in Table 3. The model-based approach in Ref. [30] has a slower calculation speed due to the higher variable dimension, with a total economic profit of 38857.31 ¥ for CSOs. The method in Ref. [16], lacking consideration for coupling constraints between variables, results in an unreliable energy plan for EVs, leading to a waste of economic benefits associated with the aggregate feasible power region of CSOs. The total economic profit for CSOs under this method is 35952.35 ¥. The data-driven method in Ref. [31], relying on a sufficient amount of data, can predict the aggregate feasible power region, and CSOs can achieve a total economic benefit of 38616.66 ¥. However, EV dispatchable potential is not a set of determined charging and discharging power vectors but an envelope space constituted by all possible charging and discharging decisions. Relying solely on a data-driven approach fails to consider the implicit constraint relationships between variables, making the resulting scheduling plan challenging to implement. In contrast, the aggregate feasible power region calculation method of CSOs in this paper has a computation time of 31.87 s, yielding a total economic profit of 39543.24 ¥ for all CSOs. The overall economic profits under the

Table 3
Results of different aggregate feasible power region calculation methods.

Method	Time (s)	Profits (RMB)				Total profits (RMB)
		CSO ₁	CSO ₂	CSO ₃	CSO ₄	
[30]	190.59	9589.08	9897.75	9646.64	9723.84	38857.31
[16]	30.12	8725.77	9377.17	8680.98	9168.43	35952.35
[31]	46.49	9543.33	9776.87	9600.97	9695.49	38616.66
This paper	31.87	9946.67	9794.75	9821.97	9979.85	39543.24

proposed method are 1.76 %, 9.99 %, and 2.40 % higher than the economic profits obtained under the methods of Refs [16,30], and [31], respectively. Therefore, the proposed method is more practical in terms of model interpretability, calculation speed, and accuracy.

5.2.2. Exactness and convergence of the model

According to Appendix A.1, the model underwent second-order cone relaxation and polyhedral approximation [51]. The accuracy of second-order cone relaxation has been proven and validated in previous literature [54]. To further verify the accuracy of the proposed model considering the inclusion of CSOs and EVs, the error metric is defined as [52]:

$$\Delta_{jk,t}^{\text{diff}} = |P_{jk,t}^2 + Q_{jk,t}^2 - \tilde{I}_{jk,t} \tilde{U}_{j,t}| \quad (13)$$

where, $P_{jk,t}$ and $Q_{jk,t}$ represent active and reactive power flow in branch jk at time t . $\tilde{U}_{j,t}$ is the voltage of node j at time t .

Fig. 10 displays the error scatter diagram of each branch in one day. Obviously, the deviation after relaxation meets the requirements of accurate operation, which is 10^6 . Additionally, Fig. 11 illustrates that the voltage deviations at each node also satisfy the constraint requirements.

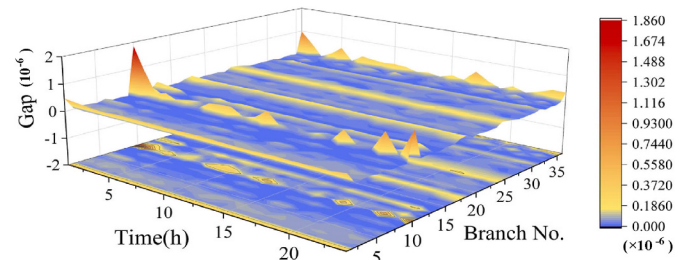


Fig. 10. Gap at each branch under different periods.

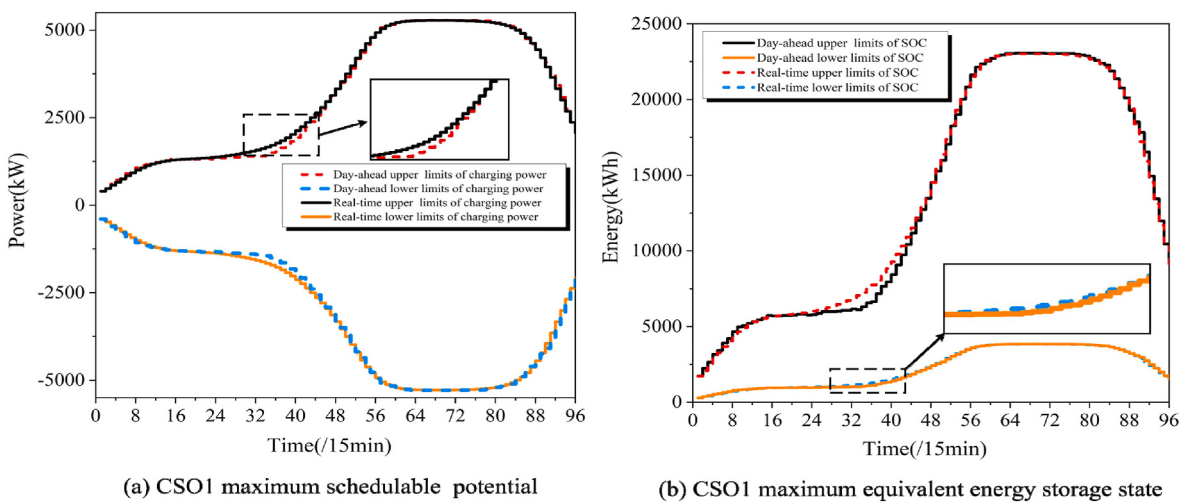


Fig. 9. Day-ahead and real-time aggregate feasible power region of CSO₁.

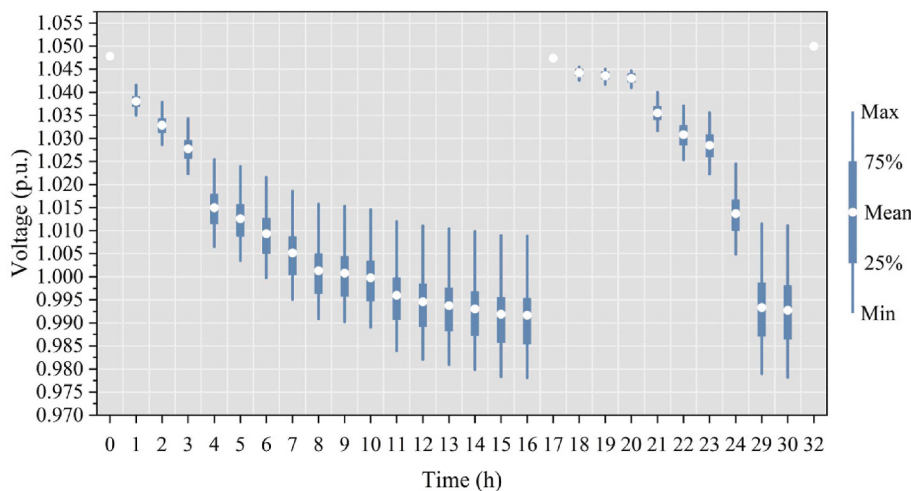


Fig. 11. Boxplot of IEEE33 distribution network node voltage.

Each CSO operates in parallel synchronization, with individual optimization runtimes kept within 40 s, ensuring compliance with the grid dispatch requirements. The convergence of the proposed distributed coordination mechanism is depicted in Fig. 12. It can be observed that convergence is achieved in approximately 17 iterations, indicating a fast convergence rate, which is acceptable.

5.2.3. Evaluation of distributed energy management effectiveness

In this section, simulation and verification of the power coordination optimization in the distributed energy management framework are conducted based on the hierarchical pricing mechanism formulated by the CSOs.

(1) Performance evaluation of distributed power optimization

To validate the technical advantages and economic value of the proposed hierarchical pricing mechanism, two widely used electricity pricing mechanisms were established as comparative cases:

- 1). Centralized dispatch mechanism: Each CSO, as part of the DSO's centralized management, is entirely dispatched by the DSO. Different CSOs at various nodes purchase and sell electricity based on the uniform DLMP set by the DSO [16].
- 2). Price-taker mechanism: DLMP for CSOs at different nodes is determined based on the DSO clearing mechanism. The DLMP for CSOs at different node locations is determined by the DSO, but each CSO can only participate in the DSO's day-ahead and real-

time electricity market as a price-taker. CSOs do not have the ability to influence the DLMP [26].

In contrast, the proposed hierarchical pricing mechanism enables CSOs at different nodes to actively participate in the determination of DLMP by the DSO. Additionally, EV users, through the demand response established in the robust retail pricing strategy of the CSO, indirectly participate in the energy management of the DSO. The results of the economic optimization for these two comparative pricing mechanisms and the hierarchical pricing mechanism are presented in Table 4.

The economic profits of each CSO consist of electricity transaction costs with the DSO and electricity consumption profits from EV users. It is evident that under the proposed hierarchical pricing mechanism, the total economic profits of CSOs (39543.24 €) are higher, with an increase of 18.60 % and 2.94 % compared to the centralized dispatch mode (33341.58 €) and price-taker mode (38415.26 €), respectively. Notably, under the proposed mechanism, CSOs can represent EV users to participate in the DLMP formulation and electricity management with the DSO, thereby yielding more economic benefits. For the DSO, the proposed mechanism can achieve lower economic costs (51875.39 €), reducing the total economic costs by 25.96 % and 27.99 % compared to the centralized dispatch mode (66394.07 €) and price-taker mode (52711.67 €), respectively. The proposed mechanism simultaneously considers the impact of the node locations of CSOs, EV demand response, and large-scale EV uncertainty on electricity price formulation. Compared to the two other payment mechanisms, CSOs under the hierarchical pricing mechanism can reduce the purchase of electricity

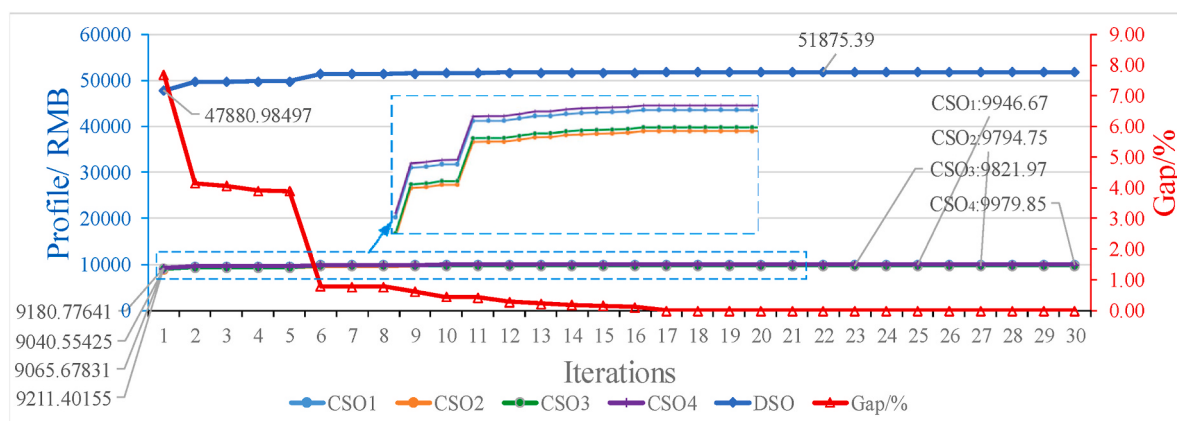


Fig. 12. Convergence curve of the proposed framework.

Table 4
Comparison of results under three different modes.

	EV users (profit/RMB)				Charging station (profit/RMB)				Distribution network (cost/RMB)				Computation time (s)
	$f_{EV_i}^{cost}$	$f_{EV_i}^{utility}$	f_{EV_i}	$f_{EV_i}^{cost}$	f_{CSO_i}	f_{CSO_i}	$\sum f_{CSO}$	f_{SO}	f_{BS}	f_{BS}	f_{BS}	f_{BSO}	
Centralized dispatch Mode	CSO ₁ -10054.51	19414.70	9360.19	-1680.25	10054.51	8374.26	33341.58	74382.60	1301.86	1680.25	66394.07	23.28	
	CSO ₂ -9839.80	18548.40	8708.60	-1494.33	9839.80	8345.47					1494.33		
	CSO ₃ -10339.58	18959.40	8619.82	-2213.98	10339.58	8125.59					2213.98		
	CSO ₄ -12398.09	21866.15	9468.06	-3901.83	12398.09	8496.26					3901.83		
Price-taker Mode	CSO ₁ -10177.21	19414.70	9237.49	-1679.25	10177.21	8497.97	38415.26	61736.82	1029.64	1679.25	52711.67	36.81	
	CSO ₂ -11240.15	18548.40	7308.25	-1514.31	11240.15	9725.84					1514.31		
	CSO ₃ -11927.37	18959.40	7032.01	-2372.48	11927.37	9554.89					2372.48		
	CSO ₄ -15125.31	21866.15	6740.84	-4488.75	15125.31	10636.56					4488.75		
This paper	CSO ₁ -11667.45	19414.70	7747.25	-1720.83	11667.45	9946.67	39543.24	60862.49	958.76	1720.83	51875.39	31.87	
	CSO ₂ -11310.07	18548.40	7238.33	-1515.32	11310.07	9794.75					1515.32		
	CSO ₃ -12215.56	18959.40	6743.84	-2393.58	12215.56	9821.97					2393.58		
	CSO ₄ -14295.97	21866.15	7570.18	-4316.12	14295.97	9979.85					4316.12		

from the DSO. Line loss costs (958.67 ¥) are also reduced by 35.8 % and 7.4 % compared to the centralized dispatch mode (1301.86 ¥) and price-taker mode (1029.64 ¥), contributing to the economic operation of the DSO. EV users actively participate in the formulation of the retail electricity prices of CSOs by pursuing demand response mechanisms that maximize their own benefits. The proposed mechanism not only enables EV users to participate in energy management through demand response mechanisms but also allows CSOs to leverage their advantages as aggregators and benefit from it. Moreover, it contributes to the benefit of the distribution network by reducing power losses and costs, achieving a win-win situation for all three participants.

(2) Internal power distribution of charge stations

To further analyze the effectiveness of the proposed energy management framework based on the aggregate feasible power regions of CSOs and the hierarchical payment mechanism, this section conducts an analysis of the internal power allocation and pricing distribution within CSOs. Fig. 13 illustrates the internal energy distribution within CSO₁ under the hierarchical payment mechanism, showcasing the power allocation among DSO, BESS, PV/Wind, and EV users. The power distribution of the 10 types of EVs within CSO₁ are demonstrated in Fig. 14. In contrast, Figs. 15 and 16 represent the internal energy distribution within CSO₁ under the centralized dispatch mode and the price-taker mode, respectively.

Based on the internal energy distribution within CSO₁ illustrated in Fig. 13 and the charging and discharging behaviors of the 10 types of EVs within the coverage area as shown in Fig. 14, the optimization results and analysis of the proposed CSOs distributed energy management based on the hierarchical pricing mechanism and the aggregate feasible power regions are outlined below:

- 1) The day-ahead and real-time DLMP and retail electricity prices are shown in Fig. 13 (b), where the retail electricity prices remain constant for multiple periods of the day, which is related to the demand response model based on the Stackelberg game. Since the follower problem of the Stackelberg model is essentially a sorting problem and cannot adequately reflect the demand elasticity of EV users, CSOs prefer to set fixed retail electricity prices to control the electricity behavior of EVs during the real-time stage.
- 2) Under the retail electricity price shown in Fig. 13(b), the charging and discharging profiles of 10 types of EVs are displayed in Fig. 14. Variations in EV preference parameters lead to diverse charging and discharging patterns. However, all EV users adhere to the pattern of “charging during off-peak hours and discharging during peak hours”. This indicates that EVs can effectively participate in demand response with CSOs through the hierarchical pricing mechanism.
- 3) In certain scenarios, CSOs engage in both day-ahead purchasing and real-time selling of electricity. This behavior arises due to the uncertainty between the electricity demand of EV users and real-time electricity prices, which compels CSOs to employ hedging strategies to maximize their expected profits. This market behavior by CSOs can be interpreted as a form of “hedging” that helps them mitigate potential losses resulting from adverse price fluctuations, thereby aiding in managing market risks.
- 4) The real-time buying and selling curves of CSOs are depicted in Fig. 13 (a). It is evident that CSOs exhibit distinct electricity trading behaviors based on the day-ahead and real-time DLMP curves. The curves demonstrate that CSOs choose to purchase electricity during low-price periods and sell excess electricity during high-price periods to maximize their profits. Additionally, the purchasing and selling volumes of CSOs satisfy the constraints of the aggregate feasible power regions, as illustrated in Fig. 7.
- 5) The charging and discharging curves of the BESS, as shown in Fig. 13 (a), exhibit a similar trend to the real-time purchasing and selling curves. This similarity is attributed to the BESS provides greater

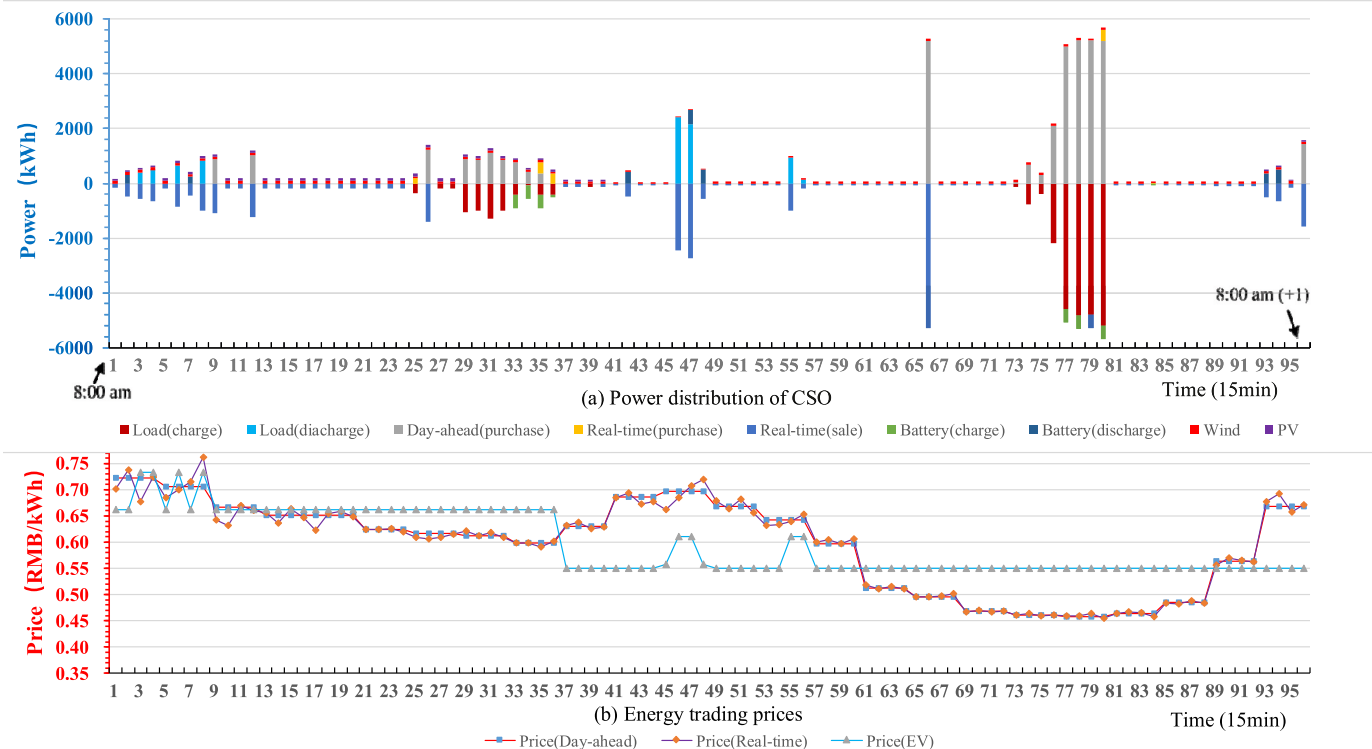


Fig. 13. Power distribution and hierarchical price inside CSO₁ (hierarchical pricing mechanism).

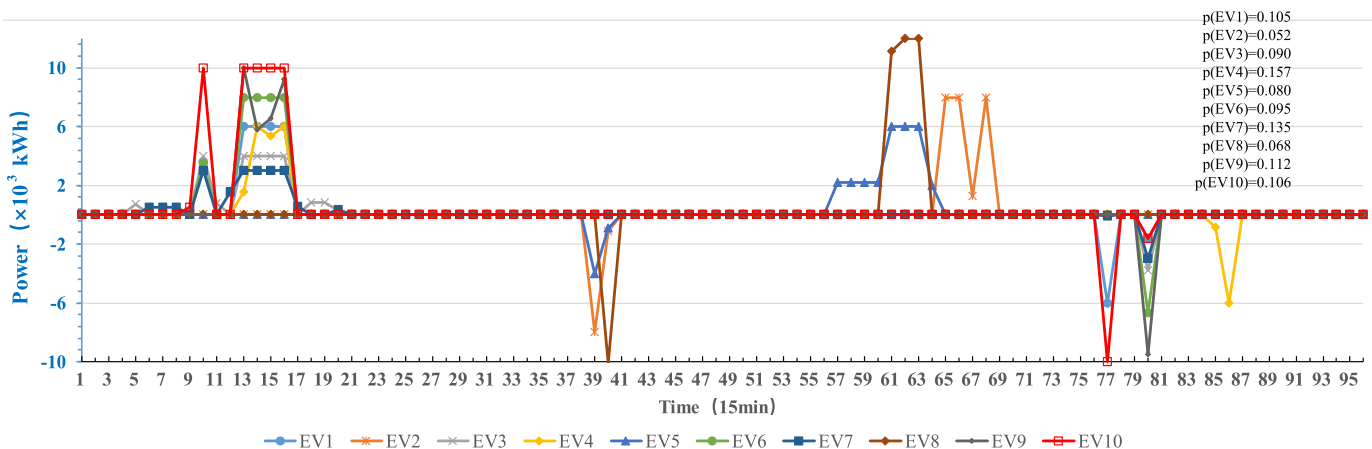


Fig. 14. Curve of charging and discharging power of different types of EVs in CSO₁.

flexibility to CSOs, allowing them to purchase electricity during low-price periods and store it for sale during high-price periods, thereby taking advantage of the time difference in electricity prices. Furthermore, the flexibility of the BESS broadens the decision space of the energy management system, helping CSOs mitigate the adverse impacts of uncertain EV electricity demand.

Further analysis was conducted on the optimized operation results under the centralized dispatch mode and the price-taker mode. Referring to the energy distribution of CSO_1 under the centralized dispatch mode corresponding to Fig. 15, the DSO formulates unified day-ahead and real-time DLMPs for transactions with various CSOs to maximize societal benefits. The DLMP set by this mode in Fig. 15(b) is lower than the pricing outcomes determined by the proposed mechanism. Based on the unified DLMP, CSOs can promptly update their energy dispatch plans and retail electricity prices, and their internally deployed BESS

engages in arbitrage through day-ahead and real-time power purchases. The internal energy distribution in Fig. 15 (a) within CSO_1 under the centralized dispatch mode aligns with the results presented in Fig. 13 (a) under the proposed mechanism. However, since DLMP is determined uniformly by the DSO, CSOs are unable to actively engage in DLMP decision-making and can only passively adjust their electricity consumption plans. Consequently, the energy management of CSOs based on the centralized dispatch mode, lacking proactive involvement of CSOs, leads to comparatively inferior economic profits (8374.26 € in comparison with 9946.67 €).

Examining the energy distribution within CSO_1 under the price-taker mode, as illustrated in Fig. 16, the DSO formulates DLMP tailored to the distinct locations of various CSOs. The DLMP of this mode falls within the range between the centralized dispatch mode and the proposed pricing mechanism. In this payment mode, CSOs are limited in demonstrating extensive electricity consumption behaviors, such as the

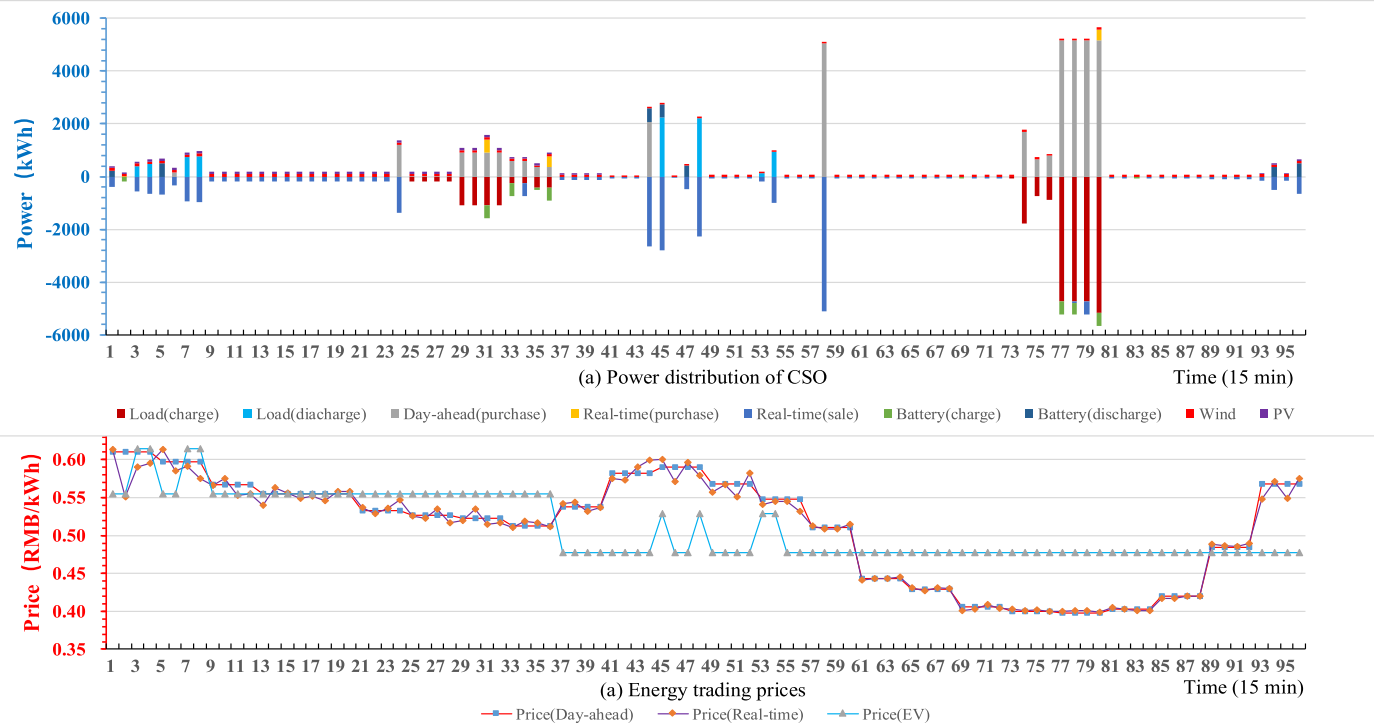


Fig. 15. Power distribution and hierarchical price inside CSO₁ (centralized dispatch mode).

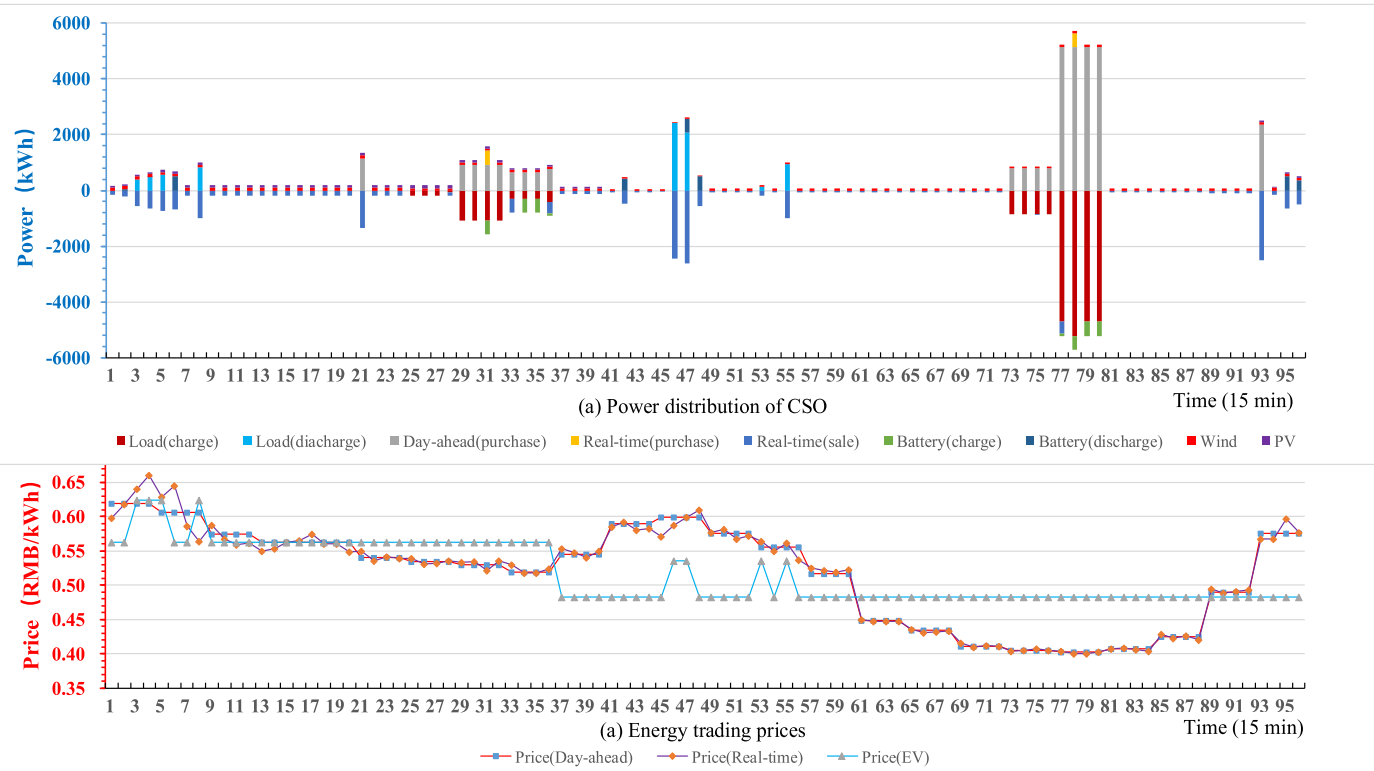


Fig. 16. Power distribution and hierarchical price inside CSO₁ (price-taker mode).

“arbitrage between day-ahead and real-time stages through low electricity prices” observed in the other two modes. This limitation arises from the constraints imposed by DSO’s unified clearing mechanism on the DLMP differentials between day-ahead and real-time power purchases. CSOs are also unable to capture significant economic profits by actively participating in the pricing decision-making process of the DSO. They can maximize profits by primarily adjusting retail electricity prices with EV users and passively adapting their scheduling plans with the DSO. Consequently, the economic profits under this mode (8497.97 ¥) are lower than the profits (9946.67 ¥) based on the proposed pricing mechanism. Both the centralized dispatch mode and the price-taker mode exhibit the ability to realize the value of EV users who actively participate in energy management and enable CSOs, as aggregators, to achieve economic optimization goals through coordinating internal BESS, PV/Wind, and EV charging/discharging plans.

Based on the characteristics of the hierarchical pricing mechanism, centralized dispatch and price-taker modes, a radar chart shown in Fig. 17 is obtained to compare the differences between the three pricing modes in terms of fairness, privacy, marketability, coordination, and robustness. Among them, fairness refers to the correlation between revenue and individual decisions. The hierarchical pricing mechanism is stronger than the price-taker mode, with the centralized scheduling mode being the least favorable; Privacy indicates the degree of confidentiality of information during the decision-making process. Both the price-taker mode and the hierarchical pricing mechanism are stronger than the centralized scheduling mode; Marketability refers to the ability to change market prices through decisions. The hierarchical pricing mechanism is stronger than the price-taker mode and the centralized scheduling mode; Coordination represents the ability of participants to cooperate. The hierarchical pricing mechanism and the centralized scheduling mode are both stronger than the price-taker mode; Robustness denotes the impact of market behavior prediction accuracy on revenue. The centralized scheduling mode is stronger than the hierarchical pricing mechanism, and the price-taker mode is the weakest.

(3) Distributed locational marginal prices analysis

Since the energy trading cost contributes to the majority of the overall profits of charging stations in both the proposed mechanism and the other two contrasting payment modes, the transaction prices behind the analysis yield intriguing insights. Fig. 18 illustrates the distribution of the DLMPs between the four charging stations and the DSO at $t = 12:00$. As described in Section 4.1.1, under the proposed mechanism, the electricity clearing prices are calculated based on the dual variables of equation (9). These prices serve as nodal marginal prices, with a clear physical interpretation that effectively reflects the value of electrical power at different bus nodes in the distribution network. They consider

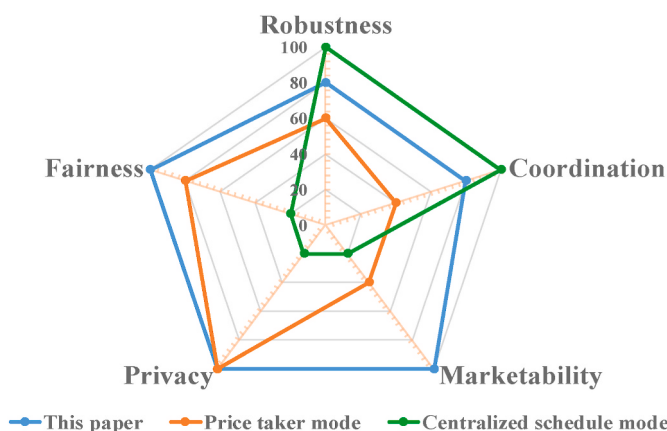


Fig. 17. Radar chart of different payment modes of CSOs.

factors such as load and generation levels, as well as the physical limitations of the distribution network transmission lines.

According to Fig. 19 (a), the DLMP trends of the four charging stations are consistent. This consistency arises because they are located within the coverage of the same DSO. Conversely, as shown in Fig. 19 (b), the two charging stations located far apart (at buses 19 and 11) and the two charging stations located close to each other (at buses 6 and 26) exhibit different and approximately similar trading price magnitudes, respectively. If the increasing marginal cost benefits are disregarded and the electricity market price is assumed to be a constant exogenous variable, a uniform clearing mechanism would amplify the marginal cost benefits of electricity production. Consequently, an equal DLMP for different CSOs, like the centralized dispatch mode, may lead to significant deviations, which can impact the market decisions of CSOs.

(4) Robust retail pricing strategy analysis

To assess the feasibility of the two-stage robust retail pricing strategy, empirical distributions are utilized as a benchmark for distributional robust optimization in this section. The distribution outcomes for various types of EVs under both approaches are depicted in Fig. 20. While there exists a certain disparity between the worst distribution obtained through robust optimization and the empirical distribution derived from clustering, no significant difference is observed. This is due to the sufficiently large number of samples used for clustering, resulting in a smaller moment distance between the actual and empirical distributions, thereby indicating that the two-stage robust optimization model does not exclusively emphasize conservatism. Contrasted with existing prediction-based general robust optimization and adaptive robustness, the two-stage robust optimization is data-driven and can balance the optimality and conservatism of the pricing strategy.

To further validate the economic value of the robust retail pricing strategy, the empirical distribution is regarded as the deterministic optimization model. The profits for CSOs under both strategies are further analyzed, as illustrated in Fig. 21. The results demonstrate that the robust pricing strategy can minimize the fluctuation range in profits for CSOs, all the while sustaining a superior average revenue compared to the deterministic model. This suggests that the robust pricing strategy takes into full account the deviation between the actual and empirical distribution, thereby expanding the strategy search range of CSOs and rendering it more universally applicable. In terms of long-term operations, the results derived from robust optimization can readily adapt to a broader array of practical scenarios, thereby enhancing the expected profits for CSOs.

5.2.4. Scalability analysis of the proposed framework

The proposed mechanism is effective even when the CSOs are located in different feeder lines. As shown in Fig. 22, in the proposed coordination mechanism: 1) CSO_1 and CSO_2 iteratively interact with the DSO in feeder A until convergence, and CSO_3 and CSO_4 iteratively interact with the DSO in feeder B until convergence; 2) Each DSO updates its strategies based solely on its own network and the buying/selling price information from the utility without needing to know the information of other DSOs. Therefore, this distributed mechanism can operate in parallel and independently when CSOs are situated at different feeders. In other scales of radial distribution networks, the proposed framework can also be modeled and solved through the classical ADMM framework. By utilizing the convex relaxation and the polyhedral approximation in Appendix A.1 and dealing with bilinear terms in equation (6), the initial problem can be transferred into a convex problem. Therefore, the proposed distributed coordination mechanism is guaranteed to converge to the centralized optimum [26].

To further demonstrate the scalability of the proposed distributed energy management framework, this study compares the computation time and the economic value for different-sized distribution networks with varying numbers of charging stations: 4, 8, 12, 16, 20, and 24. As

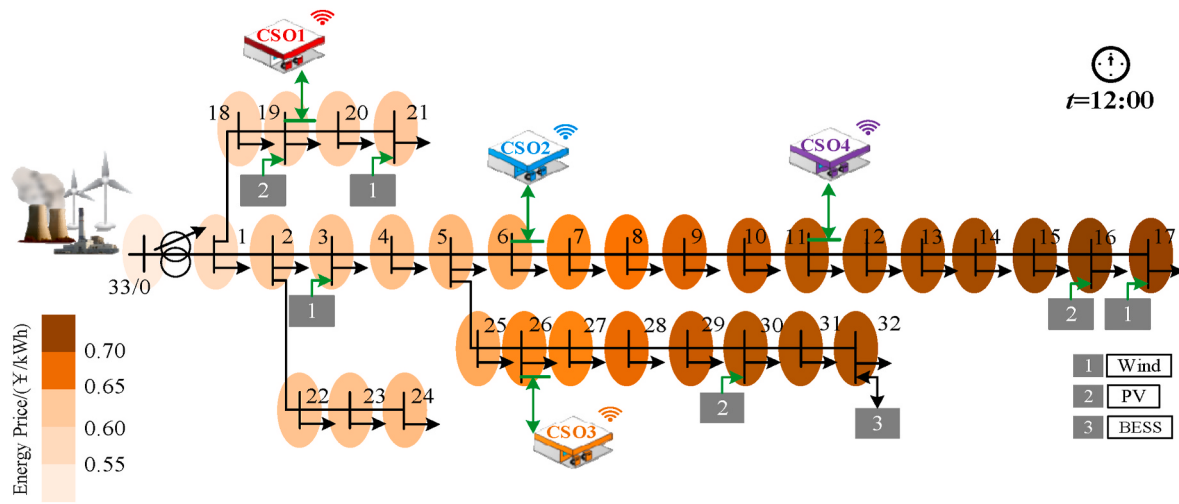


Fig. 18. Energy transaction electricity prices (DLMP) between CSOs and DSO (Case 2).

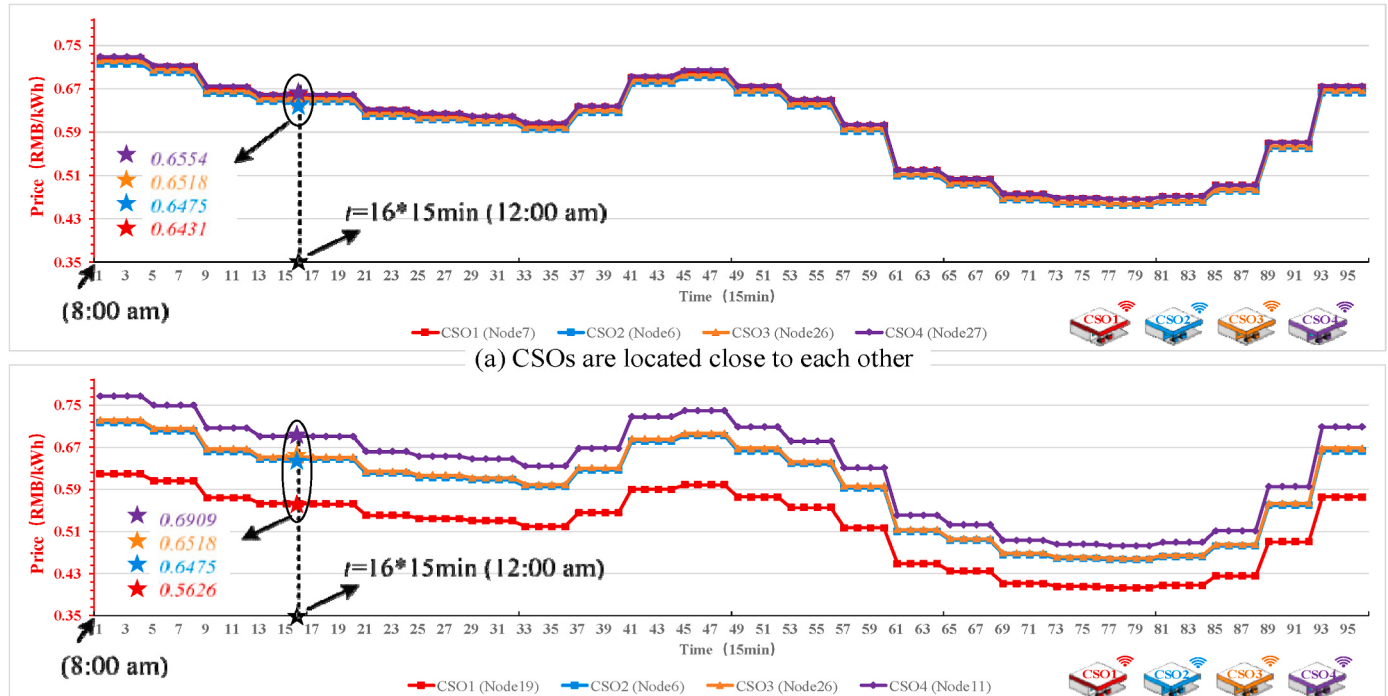


Fig. 19. Energy transaction electricity prices (DLMP).

shown in Fig. 23, in the IEEE 33 distribution network, the total computation time for CSOs and the DSO remains relatively stable with an increase in the number of charging stations, stabilizing at around 35s and 120s, respectively, with a solver gap set at 0.00 %. The computation of charging stations can be parallelized on computers, ensuring that the final computation time meets the requirements of grid scheduling. Therefore, the number of CSOs does not impact the performance of the proposed framework. For IEEE 69 and IEEE 118 node distribution networks, the computation time for both CSOs and the DSO is longer than that of the IEEE 33 distribution network but remains within the acceptable range for the grid dispatch requirements. With an increase in the number of nodes, the computation time for the DSO increases due to the increase in the number of variables in the electricity clearing model.

However, owing to the characteristics of the mixed-integer programming problem in the transferred electricity clearing model itself, the precision and efficiency of the solution can be guaranteed by employing advanced solvers [19]. The optimization results of different numbers of charging stations in various IEEE node networks are presented in Table 5. It is evident that, due to the fixed charging demands of EVs in different node networks, the total profits of CSOs show a modest upward trend with the increase in the number of charging stations. The operational costs of DSO exhibit a certain declining trend. From a practical perspective, the increased profits from expanding CSOs cannot outweigh the initial construction costs of additional charging stations. Nevertheless, the comparative results further confirm the scalability, technical value, and profit potential of the proposed operational strategy for CSOs.

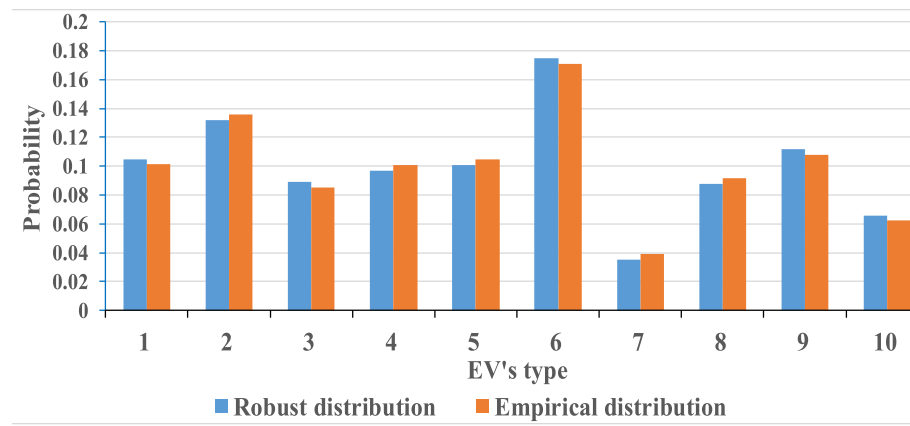


Fig. 20. Proportion of different types of EVs in different models.

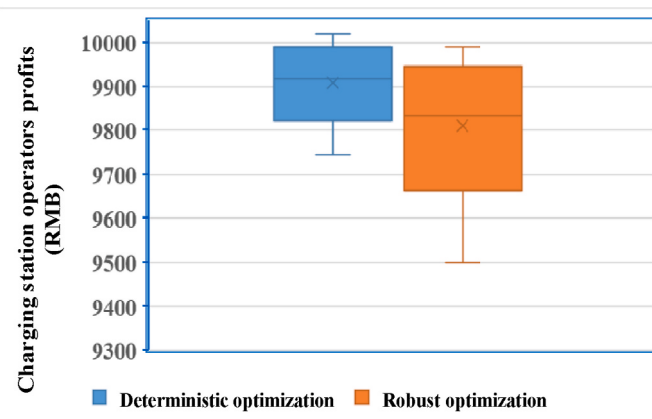


Fig. 21. Boxplot of profits in different models.

5.3. Analysis of demand response of electric vehicles

To further investigate the effectiveness of the EV demand response mechanism that contained in the proposed framework, this section provides an extended analysis of the distributed energy management framework of CSOs, focusing on two aspects: EV uncertainty and EV utility functions.

5.3.1. Uncertainty in the probability distribution of electric vehicles

According to equation (14) [60], the value of the confidence level affects the confidence set and thus the conservativeness of the framework. Taking CSO₁ as an example, the impact of confidence level (ω) on the optimization results of the charging station is examined based on equation (14). In this part, the confidence level range is set as [0.5, 0.99]. Table 6 presents the objective values and variations of the CSO optimization model. It is observed that as the confidence level increases, both the objective values and variations of the CSO optimization model increase. That is because as the confidence level increases, the confidence set becomes larger since we need to guarantee that the fuzzy distribution of large-scale EVs is in the confidence set with a higher confidence level (0.99).

$$\theta \text{ for } L_1 \text{ norm : } \theta_1 = \frac{\mathcal{N}^{EV}}{2M} \ln \frac{2\mathcal{N}^{EV}}{1 - \omega_1} \quad (14a)$$

$$\theta \text{ for } L_\infty \text{ norm : } \theta_\infty = \frac{1}{2M} \ln \frac{2\mathcal{N}^{EV}}{1 - \omega_\infty} \quad (14b)$$

where, θ_1 and θ_∞ correspond to the permissible deviation limits for probability under the constraints of the 1-norm and ∞ -norm, respectively. M denotes the number of sampled historical EV data. ω_1 and ω_∞ represent the probability confidence levels of uncertainty for equations (14a) and (14b), respectively.

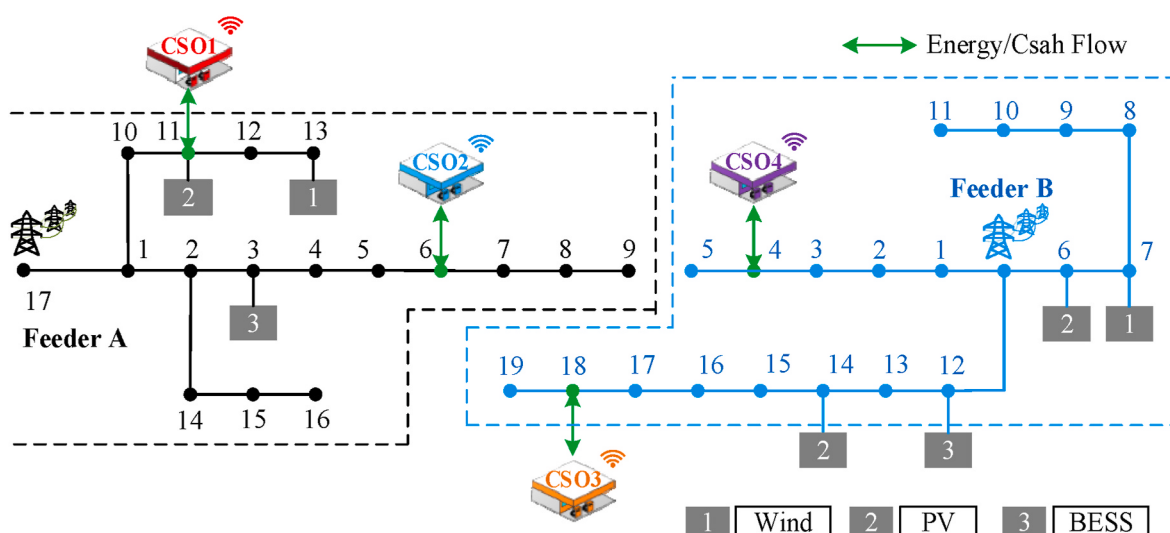


Fig. 22. Illustration of a two-feeder case.

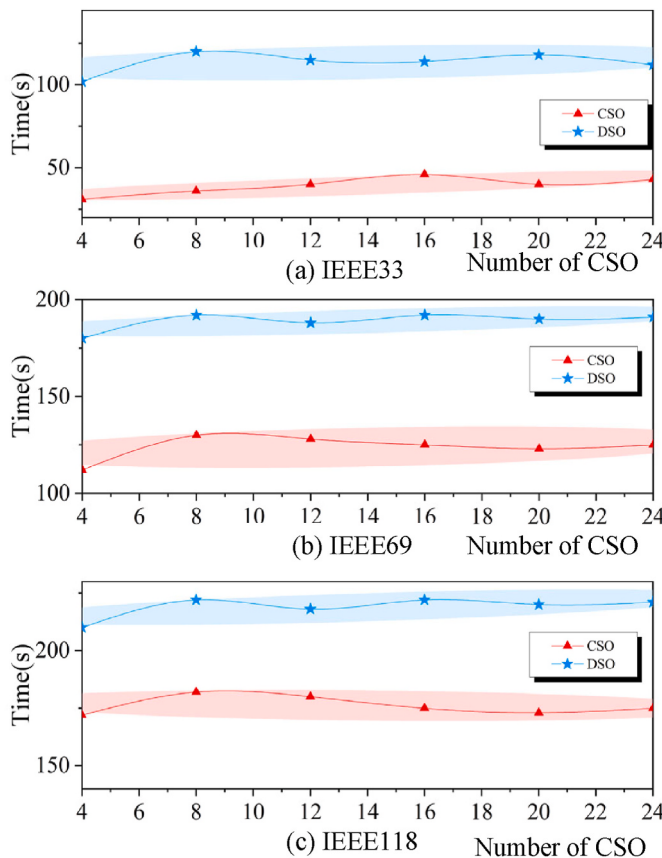


Fig. 23. Relationship between computation time and the number of CSOs in different scale of distributed network.

Table 5

Comparison of computation time and economic value with different numbers of charging stations.

Network	Number of CSOs	Computing time (s)		Total profit/cost (RMB)	
		CSOs	DSO	CSOs ($\sum f_{CSO}$)	DSO (f_{DSO})
IEEE 33	4	31	102	39543.24	51875.39
	12	40	115	42986.27	51642.84
	22	42	116	43459.73	50867.59
IEEE 69	4	112	180	48732.71	70591.07
	12	128	188	52975.87	70004.86
	22	124	190	53459.45	69758.24
IEEE 118	4	172	210	56428.24	88729.46
	12	180	218	61341.45	86687.25
	22	174	220	62007.12	85478.28

5.3.2. Impact of the economic strategy of electric vehicles

To further consider the utility function of EVs, this section explores the charging satisfaction of EVs, assuming that the unit utility of EVs,

denoted as $\{\alpha_n^{EV}\}$, decreases with time, indicating a preference for rapid charging (fast charging mode), as shown in Fig. 24. The optimization results of the proposed operational mechanism under the fast-charging mode and the before-benefits allocation method in Ref. [26] are supplemented in Table 7. In comparison with Tables 4 and in the fast-charging mode, the total economic profit of CSOs (36487.03 ¥) is 7.23 % lower than the economic profit under constant EV utility value (39543.24 ¥). The total profit of EV users within the coverage area of each charging station (28708.47 ¥) is 2.65 % lower than that under constant utility value (29299.60 ¥). This indicates that, although the "fast charging mode" meets the needs of EV users, it has an adverse impact on overall economic benefits. To further validate the financial benefit allocation to engage EVs in participating in the proposed economic strategy, the before-benefits allocation method is supplemented as a comparative case in this section. The total profit of CSOs under the proposed strategy was the highest (39543.24 ¥), followed by the figures for the before-benefits allocation method and the fast-charging mode (36839.13 ¥ in comparison with 36487.03 ¥). Compared with the profit of DSO under the proposed strategy (51875.39 ¥), the profits of DSO under the before-benefits allocation method and fast charging mode are 75898.47 ¥ and 78401.29 ¥, respectively. It can be seen that the profits of EVs covered by each charging station, each CSO and DSO are no more than those under the proposed strategy, compared with Tables 3 and 7. Hence, EV users, CSOs and DSO are all willing to participate in the proposed management scheme.

By comparing Figs. 13 and 24, it is evident that the change in the EV utility function causes EV users to seek rapid charging while maximizing their own benefits, resulting in an advancement of EV charging time by approximately 1 h. As depicted in Fig. 24 (b), it is evident that, in order to derive more revenue from EV users, both the retail electricity prices set by CSOs and the DLMP formulated by the DSO will track changes in the utility function of EV users. Compared to the results of fast charging mode, the proposed retail electricity pricing strategy for EVs increases the utility value of EV users by 2.65 %. However, the adoption of fast charging mode has an adverse impact on the total economic revenue of EV users, reducing it from 29299.60 ¥ to 28708.47 ¥. This pricing strategy balances the economic profits of both EV users and CSOs, effectively mitigating market risks arising from EV users and electricity market uncertainties and fully unleashing the demand response potential of EV users as flexible load units. It demonstrates the effectiveness and practicality of the robust retail pricing mechanism between CSOs and EV users and the power clearing mechanism between the DSO and CSOs embedded in the hierarchical pricing mechanism.

6. Conclusion

A novel distributed energy management framework for CSOs in the distribution network is designed in this study. The aggregate feasible power regions of CSOs are computed using a new method based on the combination of Minkowski summation and the data-driven approach, facilitating participation in the optimized resource allocation of the DSO. Furthermore, this paper proposes a hierarchical pricing mechanism among the DSO, CSOs, and EV users with a clear physical

Table 6
Effects of confidence set on results.

ω	Profits (RMB)					Total profits (RMB)
	CSO ₁	CSO ₂	CSO ₃	CSO ₄	θ	
↑	0.50	10078.69	9924.75	9952.34	10112.31	40068.09
	0.60	10056.57	9902.97	9930.49	10090.11	39980.13
	0.70	10034.49	9881.23	9908.69	10067.96	39892.37
	0.80	10012.46	9859.54	9886.94	10045.86	39804.80
	0.90	9990.48	9837.89	9865.23	10023.81	39717.42
	0.95	9968.55	9816.30	9843.58	10001.81	39630.24
	0.99	9946.67	9794.75	9821.97	9979.85	39543.24

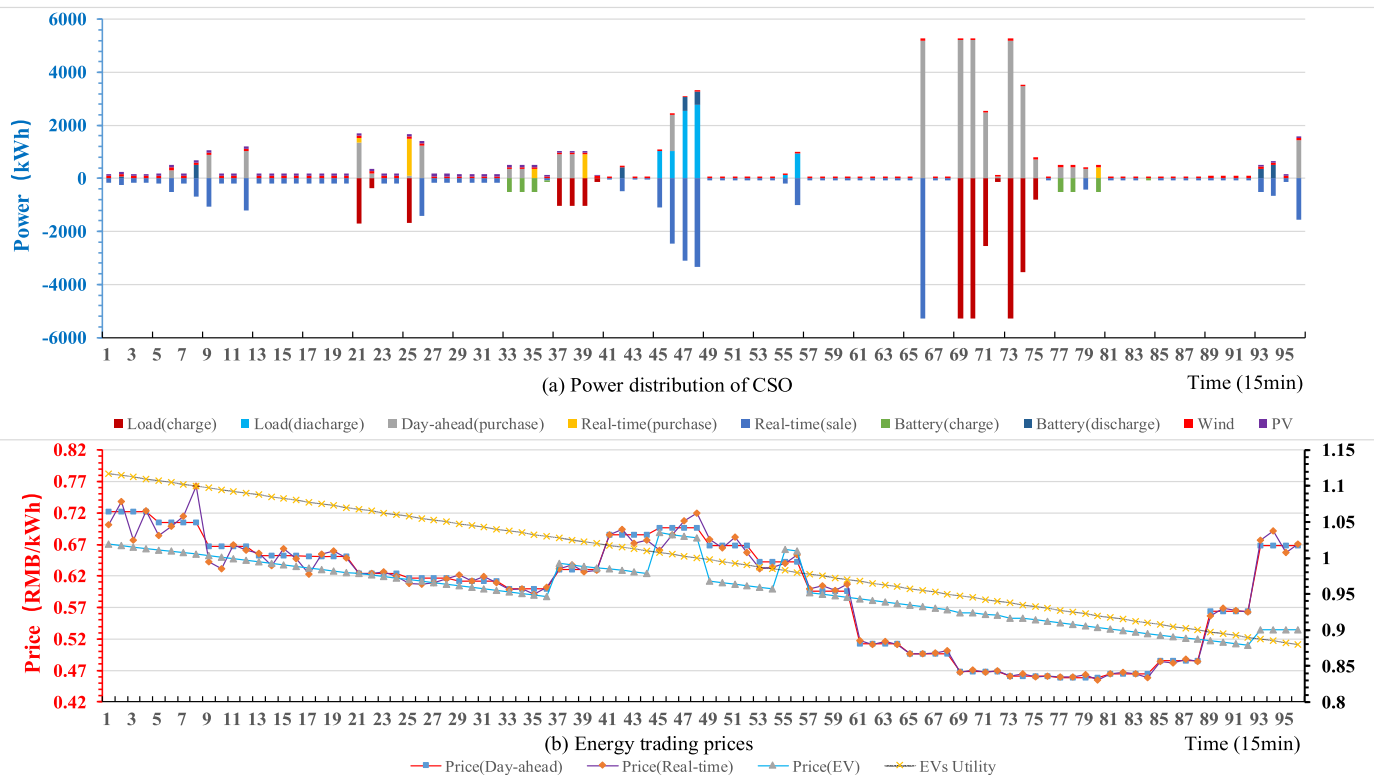


Fig. 24. Power distribution and hierarchical price inside CSO₁ (fast charging mode).

interpretation. This payment mechanism comprises two components: the clearing electricity pricing mechanism between CSOs and the DSO, and the retail electricity pricing mechanism between EV users and CSOs. This framework thoroughly considers the electricity market clearing mechanism of the DSO and the demand response of EV users, ultimately employing ADMM distributed optimization methods for resolution. Some conclusions are drawn as follows:

- (1) The proposed method for calculating the aggregate feasible power regions of CSOs highlights the advantages of both model-based and data-driven methodologies. Minkowski summation compresses the EV cluster into a virtual energy storage device, reducing model dimensions while preserving inter-variable constraints. The data-driven scheme embodies the impact of unknown factors implicit in a wealth of historical data on the aggregate feasible power regions. Experimental results demonstrate that the proposed method outperforms alternative competitive methods in terms of both precision and speed. Compared to the model-based method, the total economic profits for CSOs under the proposed method increased by 1.77 %, reaching 39543.24 € in contrast to 38857.31 €. When compared to the data-driven method, the total economic profits for CSOs under the proposed method increased by 2.40 %, amounting to 39543.24 € in contrast to 38616.66 €.
- (2) The hierarchical pricing mechanism among the DSO, CSOs, and EV users provides a novel perspective for energy transaction patterns. EV users can actively engage in the decision-making process of retail electricity prices and gain significant economic profits through the demand response mechanism, rather than passively accepting fixed retail prices. The two-stage robust retail pricing strategy of CSOs effectively captures the utility of EV users and addresses the uncertainties associated with EVs. Moreover, leveraging the aggregated power dispatchable potential, CSOs can participate as contributors in the DSO's clearing market, influencing the DLMP and reaping substantial benefits, as

opposed to passive involvement in the DSO's transaction market through centralized scheduling and price-taker models. The proposed hierarchical pricing mechanism can achieve superior economic profits for CSOs compared to traditional centralized dispatch and price-taker modes. The total economic profit amounts to 39543.24 €, marking a significant 18.6 % increase compared to the profit of the centralized dispatch mode (33341.58 €) and a 2.94 % increase compared to the price-taker mode (38415.26 €). Due to the reasonable internal energy distribution within CSOs, the DSO experiences a notable reduction in overall economic operating costs by 25.96 % and 27.99 %, along with a decrease in line loss costs by 35.8 % and 7.4 %, thereby ensuring the technological and economic feasibility of the DSO.

- (3) Within the coverage area of the DSO, each CSO operates independently and in parallel through the transformed distributed optimization mechanism, which can achieve precise and rapid model solving. Across various scales of radial distribution networks (IEEE 33, 69, and 118), as the number of CSOs increases from 4 to 24, the optimization computation time for CSOs and the DSO tends to stabilize, meeting the grid dispatch requirements within 5 min. The operational results indicate that the precision of the approximation scheme in this paper meets the practical operational requirements of the power grid. Furthermore, the independent operation of each CSO and the DSO, employing the distributed optimization approach (ADMM) with a clear physical interpretation, ensures the privacy of EV user data compared to centralized dispatch modes and reflects the mutual impact of DSO, CSOs, and EVs in real-world scenarios.

In real-world applications, the proposed distributed energy management framework can serve as a technical reference for the energy management of CSOs within distribution networks. The proposed pricing mechanism, being insensitive to the number of charging stations, holds technological value for optimized management in future scenarios.

	EV users (profit/RMB)						Charging station (profit/RMB)						Distribution network (cost/RMB)						Computation time (s)
	$f_{EV_i}^{\text{cost}}$	$f_{EV_i}^{\text{utility}}$	f_{EV_i}	f_{gi}	$f_{EV_i}^{\text{cost}}$	f_{CSO}	$\sum f_{CSO}$	f_{TSO}	f_{loss}	f_{gi}	f_{BSO}								
Fast charging mode	CSO ₁ -11361.01	18449.14	7088.13	-1989.00	11361.01	9372.01	36487.03	65722.38	1176.89	1989.00	78401.29	39.48							
	CSO ₂ -10961.80	17799.61	6837.83	-1861.29	10961.80	9100.51													
Before-benefits allocation	CSO ₃ -11560.70	18609.29	7048.59	-2773.61	11560.70	8787.09						2773.61							
	CSO ₄ -14105.57	21839.49	7733.92	-4878.15	14105.57	9227.42													
	CSO ₁ -11427.75	18704.70	7276.95	-1977.45	11427.75	9450.30	36839.13	63591.54	1063.76	1977.45	75898.47	42.59							
	CSO ₂ -10111.20	17976.60	6965.40	-1816.70	11011.20	9194.50													
	CSO ₃ -11616.64	18715.78	7099.14	-2730.79	11616.64	8895.85						1816.70							
	CSO ₄ -14026.71	21792.82	7766.11	-4718.23	14026.71	9308.48													
												4718.23							

Table 7
Optimization result of fast charging mode and before-benefits allocation method.

involving multiple CSOs. The optimization principles of ADMM can extend this energy management framework to multiple distribution network scenarios, enabling unified energy management across different CSOs. EV users can actively participate in the energy trading process with the grid by relying on CSOs through the demand response mechanism. The proposed payment mechanism among the DSO, CSOs, and EV users effectively harnesses the potential economic value of all three participants, achieving overall optimization at the distribution network level.

In future research, the energy sharing mechanisms and the electricity bidding models among various CSOs will be explored. By investigating the game processes among CSOs under incomplete information, potential economic value among CSOs will be sought. Additionally, a comprehensive study of the linkage mechanisms between the day-ahead and the real-time electricity market in the clearing model of the DSO will be undertaken. The aim is to delve into the impact of numerous uncertainties in the real-time electricity market on electricity pricing mechanisms, establishing a more robust retail electricity pricing strategy. Furthermore, considerations will be extended to incorporate constraints within the transportation network where EV users operate. Simultaneously, refined optimization models and operational mechanisms will be developed to capture the interaction between CSOs and the distribution network, as well as the transportation network relevant to EV users.

CRediT authorship contribution statement

Weiqi Meng: Conceptualization, Data curation, Methodology, Resources, Supervision, Writing – review & editing. **Dongran Song:** Conceptualization, Investigation, Methodology, Software, Writing – original draft. **Liansheng Huang:** Methodology, Resources, Supervision, Writing – review & editing. **Xiaojiao Chen:** Methodology, Resources, Supervision, Writing – review & editing. **Jian Yang:** Investigation, Writing – review & editing. **Mi Dong:** Supervision, Writing – review & editing. **M. Talaat:** Writing – review & editing. **M.H. Elkholly:** Writing – review & editing.

Declaration of competing interest

The authors declare that they have no known competing financial interests or personal relationships that could have appeared to influence the work reported in this paper.

Data availability

No data was used for the research described in the article.

Acknowledgments

This work is supported by the National Natural Science Foundation of China under Grant 52177204; and the Major Science and Technology Projects in Anhui Province under Grant 202003a05020019.

Appendix A. Supplementary data

Supplementary data to this article can be found online at <https://doi.org/10.1016/j.energy.2024.130332>.

References

- [1] IEA. Global EV outlook 2023. Paris: IEA; 2023. <https://www.iea.org/reports/global-ev-outlook-2023>.
- [2] Chen X, Zhang H, Xu Z, Nielsen CP, McElroy MB, Lv J. Impacts of fleet types and charging modes for electric vehicles on emissions under different penetrations of wind power. Nat Energy 2018;3(5):413–21. <https://doi.org/10.1038/s41560-018-0133-0>.

- [3] Harsh P, Das D. Optimal coordination strategy of demand response and electric vehicle aggregators for the energy management of reconfigured grid-connected microgrid. *Renew Sustain Energy Rev* 2022;160. <https://doi.org/10.1016/j.rser.2022.112251>.
- [4] Fang X, Wang Y, Dong W, Yang Q, Sun S. Optimal energy management of multiple electricity-hydrogen integrated charging stations. *Energy* 2023;262. <https://doi.org/10.1016/j.energy.2022.125624>.
- [5] Powell S, Cezar GV, Min L, Azevedo IML, Rajagopal R. Charging infrastructure access and operation to reduce the grid impacts of deep electric vehicle adoption. *Nat Energy* 2022;7(10):932–45. <https://doi.org/10.1038/s41560-022-01105-7>.
- [6] Ai X, Wu J, Hu J, Yang Z, Yang G. Distributed congestion management of distribution networks to integrate prosumers energy operation. *IET Gener Transm Distrib* 2020;14(15):2988–96. <https://doi.org/10.1049/iet-gtd.2019.1110>.
- [7] Rana R, Mishra S. Day-ahead scheduling of electric vehicles for overloading management in active distribution system via web-based application. *IEEE Syst J* 2019;13(3):3422–32. <https://doi.org/10.1109/JSYST.2018.2851618>.
- [8] Parag Y, Sovacool BK. Electricity market design for the prosumer era. *Nat Energy* 2016;1(4):16032. <https://doi.org/10.1038/nenergy.2016.32>.
- [9] Yi T, Cheng X, Peng P. Two-stage optimal allocation of charging stations based on spatiotemporal complementarity and demand response: a framework based on MCS and DBPSO. *Energy* 2022;239. <https://doi.org/10.1016/j.energy.2021.122261>.
- [10] Zheng B, Wei W, Chen Y, Wu Q, Mei S. A peer-to-peer energy trading market embedded with residential shared energy storage units. *Appl Energy* 2022;308:118400. <https://doi.org/10.1016/j.apenergy.2021.118400>.
- [11] Tushar W, Chai B, Yuen C, Smith DB, Wood KL, Yang Z, et al. Three-party energy management with distributed energy resources in smart grid. *IEEE Trans Ind Electron* 2014;62(4):2487–98. <https://doi.org/10.1109/TIE.2014.2341556>.
- [12] Liu N, Yu X, Wang C, Wang J. Energy sharing management for microgrids with PV prosumers: a Stackelberg game approach. *IEEE Trans Ind Inf* 2017;13(3):1088–98. <https://doi.org/10.1109/TII.2017.2654302>.
- [13] Chen Y, Zhao C, Low SH, Wierman A. An energy sharing mechanism considering network constraints and market power limitation. *IEEE Trans Smart Grid* 2022. <https://doi.org/10.1109/TSG.2022.3198721>.
- [14] Huang X, Lin Y, Lim MK, Zhou F, Liu F. Electric vehicle charging station diffusion: an agent-based evolutionary game model in complex networks. *Energy* 2022;257. <https://doi.org/10.1016/j.energy.2022.124700>.
- [15] Li G, Yang J, Hu Z, Zhu X, Xu J, Sun Y, et al. A novel price-driven energy sharing mechanism for charging station operators. *Energy Econ* 2023;118:106518. <https://doi.org/10.1016/j.eneco.2023.106518>.
- [16] He L, Yang J, Yan J, Tang Y, He H. A bi-layer optimization based temporal and spatial scheduling for large-scale electric vehicles. *Appl Energy* 2016;168:179–92. <https://doi.org/10.1016/j.apenergy.2016.01.089>.
- [17] Tushar W, Saha TK, Yuen C, Morstyn T, Nahid Al M, Poor HV, et al. Grid influenced peer-to-peer energy trading. *IEEE Trans Smart Grid* 2020;11(2):1407–18. <https://doi.org/10.1109/TSG.2019.2937981>.
- [18] Yan Q, Zhang B, Kezunovic M. Optimized operational cost reduction for an EV charging station integrated with battery energy storage and PV generation. *IEEE Trans Smart Grid* 2019;10(2):2096–106. <https://doi.org/10.1109/TSG.2017.2788440>.
- [19] Song D, Meng W, Dong M, Yang J, Wang J, Chen X, et al. A critical survey of integrated energy system: summaries, methodologies and analysis. *Energy Convers Manag* 2022;266:115863. <https://doi.org/10.1016/j.enconman.2022.115863>.
- [20] Liu N, Wang J, Wang L. Hybrid energy sharing for multiple microgrids in an integrated heat-electricity energy system. *IEEE Trans Sustain Energy* 2019;10(3):1139–51. <https://doi.org/10.1109/TSTE.2018.2861986>.
- [21] Tushar W, Saha TK, Yuen C, Smith D, Poor HV. Peer-to-Peer trading in electricity networks: an overview. *IEEE Trans Smart Grid* 2020;11(4):3185–200. <https://doi.org/10.1109/TSG.2020.2969657>.
- [22] Zhang J, Che L, Wan X, Shahidehpour M. Distributed hierarchical coordination of networked charging stations based on peer-to-peer trading and EV charging flexibility quantification. *IEEE Trans Power Syst* 2022;37(4):2961–75. <https://doi.org/10.1109/TPWRS.2021.3123351>.
- [23] Maneesha A, Swarup KS. A survey on applications of Alternating Direction Method of Multipliers in smart power grids. *Renew Sustain Energy Rev* 2021;152:111687. <https://doi.org/10.1016/j.rser.2021.111687>.
- [24] Guo Z, Pinson P, Wu Q, Chen S, Yang Q, Yang Z. An asynchronous online negotiation mechanism for real-time peer-to-peer electricity markets. *IEEE Trans Power Syst* 2022;37(3):1868–80. <https://doi.org/10.1109/TPWRS.2021.3111869>.
- [25] Das HS, Rahman MM, Li S, Tan CW. Electric vehicles standards, charging infrastructure, and impact on grid integration: a technological review. *Renew Sustain Energy Rev* 2020;120. <https://doi.org/10.1016/j.rser.2019.109618>.
- [26] Yan D, Ma C, Chen Y. Distributed coordination of charging stations considering aggregate EV power flexibility. *IEEE Trans Sustain Energy* 2022;14(1):356–70. <https://doi.org/10.1109/TSTE.2022.3213173>.
- [27] Zhao Z, Lee CKM, Hua J. EV charging station deployment on coupled transportation and power distribution networks via reinforcement learning. *Energy* 2023;267. <https://doi.org/10.1016/j.energy.2022.126555>.
- [28] shafiei M, Ghasemi-Marzbali A. Electric vehicle fast charging station design by considering probabilistic model of renewable energy source and demand response. *Energy* 2023;267. <https://doi.org/10.1016/j.energy.2022.126545>.
- [29] LaMonaca S, Ryan L. The state of play in electric vehicle charging services – a review of infrastructure provision, players, and policies. *Renew Sustain Energy Rev* 2022;154. <https://doi.org/10.1016/j.rser.2021.111733>.
- [30] Wen Y, Hu Z, You S, Duan X. Aggregate feasible region of DERs: exact formulation and approximate models. *IEEE Trans Smart Grid* 2022;13(6):4405–23. <https://doi.org/10.1109/tsg.2022.3179998>.
- [31] Zhang Q, Wu X, Deng X, Huang Y, Li C, Wu J. Bidding strategy for wind power and Large-scale electric vehicles participating in Day-ahead energy and frequency regulation market. *Appl Energy* 2023;341. <https://doi.org/10.1016/j.apenergy.2023.121063>.
- [32] Mao M, Zhang S, Chang L, Hatzigaryiou ND. Schedulable capacity forecasting for electric vehicles based on big data analysis. *Journal of Modern Power Systems and Clean Energy* 2019;7(6):1651–62. <https://doi.org/10.1007/s40565-019-00573-3>.
- [33] Luo L, Wu Z, Gu W, Huang H, Gao S, Han J. Coordinated allocation of distributed generation resources and electric vehicle charging stations in distribution systems with vehicle-to-grid interaction. *Energy* 2020;192. <https://doi.org/10.1016/j.energy.2019.116631>.
- [34] Zhu X, Sun Y, Yang J, Zhan X, Wu F, Fan H, et al. Hierarchical management strategy for electric vehicles charging schedule considering the scarcity of charging resources. *IET Gener Transm Distrib* 2022;16(15):3092–108. <https://doi.org/10.1049/gtd2.12503>.
- [35] Adetunji KE, Hofsjer IW, Abu-Mahfouz AM, Cheng L. An optimization planning framework for allocating multiple distributed energy resources and electric vehicle charging stations in distribution networks. *Appl Energy* 2022;322. <https://doi.org/10.1016/j.apenergy.2022.119513>.
- [36] Ahsan F, Dana NH, Sarker SK, Li L, Muyeen SM, Ali MF, et al. Data-driven next-generation smart grid towards sustainable energy evolution: techniques and technology review. *Protection and Control of Modern Power Systems* 2023;8(1):43. <https://doi.org/10.1186/s41601-023-00319-5>.
- [37] Meng W, Song D, Huang L, Chen X, Yang J, Dong M, et al. A Bi-level optimization strategy for electric vehicle retailers based on robust pricing and hybrid demand response. *Energy* 2024;289:129913. <https://doi.org/10.1016/j.energy.2023.129913>.
- [38] Wu Y, Ravey A, Chrenko D, Miraoui A. Demand side energy management of EV charging stations by approximate dynamic programming. *Energy Convers Manag* 2019;196:878–90. <https://doi.org/10.1016/j.enconman.2019.06.058>.
- [39] Hu J, Morais H, Sousa T, Lind M. Electric vehicle fleet management in smart grids: a review of services, optimization and control aspects. *Renew Sustain Energy Rev* 2016;56:1207–26. <https://doi.org/10.1016/j.rser.2015.12.014>.
- [40] Yin W, Wen T, Zhang C. Cooperative optimal scheduling strategy of electric vehicles based on dynamic electricity price mechanism. *Energy* 2023;263:125627. <https://doi.org/10.1016/j.energy.2022.125627>.
- [41] Zou S, Ma Z, Yang N. Decentralized hierarchical coordination of electric vehicles in multi-microgrid systems. *IET Generation, Transm Distrib* 2019;13(13):2899–906. <https://doi.org/10.1049/iet-gtd.2018.6767>.
- [42] Asrari A, Ansari M, Khazaee J, Fajri P. A market framework for decentralized congestion management in smart distribution grids considering collaboration among electric vehicle aggregators. *IEEE Trans Smart Grid* 2020;11(2):1147–58. <https://doi.org/10.1109/TSG.2019.2932695>.
- [43] Dai W, Wang C, Goh HH, Zhao J, Jian J. Hosting capacity evaluation method for power distribution networks integrated with electric vehicles. *Journal of Modern Power Systems and Clean Energy* 2023;11(5):1564–75. <https://doi.org/10.35833/MPC.E.2022.000515>.
- [44] Xu B, Zhang G, Li K, Li B, Chi H, Yao Y, et al. Reactive power optimization of a distribution network with high-penetration of wind and solar renewable energy and electric vehicles. *Protection and Control of Modern Power Systems* 2022;7(1):51. <https://doi.org/10.1186/s41601-022-00271-w>.
- [45] Perez-Diaz A, Gerding E, McGrarty F. Coordination and payment mechanisms for electric vehicle aggregators. *Appl Energy* 2018;212:185–95. <https://doi.org/10.1016/j.apenergy.2017.12.036>.
- [46] Zhang K, Xu L, Ouyang M, Wang H, Lu L, Li J, et al. Optimal decentralized valley-filling charging strategy for electric vehicles. *Energy Convers Manag* 2014;78:537–50. <https://doi.org/10.1016/j.enconman.2013.11.011>.
- [47] Kapoor A, Patel VS, Sharma A, Mohapatra A. Centralized and decentralized pricing strategies for optimal scheduling of electric vehicles. *IEEE Trans Smart Grid* 2022;13(3):2234–44. <https://doi.org/10.1109/TSG.2022.3141261>.
- [48] Jia Z, Li J, Zhang XP, Zhang R. Review on optimization of forecasting and coordination strategies for electric vehicle charging. *Journal of Modern Power Systems and Clean Energy* 2023;11(2):389–400. <https://doi.org/10.35833/MPC.E.2021.000777>.
- [49] Jing R, Xie MN, Wang FX, Chen LX. Fair P2P energy trading between residential and commercial multi-energy systems enabling integrated demand-side management. *Appl Energy* 2020;262:114551. <https://doi.org/10.1016/j.apenergy.2020.114551>.
- [50] Yan D, Chen Y. A distributed online algorithm for promoting energy sharing between EV charging stations. *IEEE Trans Smart Grid* 2022. <https://doi.org/10.1109/TSG.2022.3203522>.
- [51] Farivar M, Low SH. Branch flow model: relaxations and convexification—Part I. *IEEE Trans Power Syst* 2013;28(3):2554–64. <https://doi.org/10.1109/TPWRS.2013.2255317>.
- [52] Farivar M, Low SH. Branch flow model: relaxations and convexification—Part II. *IEEE Trans Power Syst* 2013;28(3):2565–72. <https://doi.org/10.1109/TPWRS.2013.2255318>.
- [53] Meng W, Song D, Deng X, Dong M, Yang J, Rizk-Allah RM, et al. Dynamic optimal power flow of active distribution network based on LSOCR and its application scenarios. *Electronics* 2023;12(7):1530. <https://doi.org/10.3390/electronics12071530>.

- [54] Low SH. Convex relaxation of optimal power flow—Part II: exactness. *IEEE Transactions on Control of Network Systems* 2014;1(2):177–89. <https://doi.org/10.1109/TCNS.2014.2323634>.
- [55] Ben-Tal A, Nemirovski A. On polyhedral approximations of the second-order cone. *Math Oper Res* 2001;26(2):193–205. <http://www.jstor.org/stable/3690614>.
- [56] Bai L, Wang J, Wang C, Chen C, Li F. Distribution locational marginal pricing (DLMP) for congestion management and voltage support. *IEEE Trans Power Syst* 2017;33(4):4061–73. <https://doi.org/10.1109/TPWRS.2017.2767632>.
- [57] Qi T, Ye C, Zhao Y, Li L, Ding Y. Deep reinforcement learning based charging scheduling for household electric vehicles in active distribution network. *Journal of Modern Power Systems and Clean Energy* 2023;11(6):1890–901. <https://doi.org/10.35833/MPCE.2022.000456>.
- [58] Mahmud K, Town GE, Morsalin S, Hossain MJ. Integration of electric vehicles and management in the internet of energy. *Renew Sustain Energy Rev* 2018;82:4179–203. <https://doi.org/10.1016/j.rser.2017.11.004>.
- [59] Low SH. Convex relaxation of optimal power flow—Part I: formulations and equivalence. *IEEE Transactions on Control of Network Systems* 2014;1(1):15–27. <https://doi.org/10.1109/TCNS.2014.2309732>.
- [60] Zhao C, Guan Y. Data-driven stochastic unit commitment for integrating wind generation. *IEEE Trans Power Syst* 2015;31(4):2587–96. <https://doi.org/10.1109/TPWRS.2015.2477311>.
- [61] Neyestani N, Damavandi MY, Shafie-Khah M, Bakirtzis AG, Catalao JP. Plug-in electric vehicles parking lot equilibria with energy and reserve markets. *IEEE Trans Power Syst* 2016;32(3):2001–16. <https://doi.org/10.1109/TPWRS.2016.2609416>.
- [62] Laws ND, Hanusanto GA. Linearizing bilinear products of shadow prices and dispatch variables in bilevel problems for optimal power system planning and operations. *IEEE Trans Power Syst* 2023;38(1):668–80. <https://doi.org/10.1109/tpwrs.2022.3156475>.
- [63] Wang Y, Chen Q, Kang C. *Smart meter data analytics*. Springer; 2020.
- [64] Baran ME, Wu FF. Network reconfiguration in distribution systems for loss reduction and load balancing. *IEEE Trans Power Deliv* 1989;4(2):1401–7. <https://doi.org/10.1109/61.25627>.
- [65] Anand R, Aggarwal D, Kumar V. A comparative analysis of optimization solvers. *J Stat Manag Syst* 2017;20(4):623–35. <https://doi.org/10.1080/09720510.2017.1395182>.
- [66] Yan Q, Zhang B, Kezunovic M. Optimized operational cost reduction for an EV charging station integrated with battery energy storage and PV generation. *IEEE Trans Smart Grid* 2018;10(2):2096–106. <https://doi.org/10.1109/TSG.2017.2788440>.
- [67] Laboratory NRE. National solar and wind generation data. National Renewable Energy Laboratory; 2022. <https://www.nrel.gov/research/data-tools.html>.
- [68] Ouyang Jinxin, Yu Jianfeng, Long Xiaoxuan, Diao Yanbo, Wang Jian. Coordination control method to block cascading failure of a renewable generation power system under line dynamic security. *Protection and Control of Modern Power Systems* 2023;8(1):194–204. <https://doi.org/10.1186/s41601-023-00283-0>.